EXCIPIENT PHASE BEHAVIOR IN THE FREEZE-CONCENTRATE

A THESIS
SUBMITTED TO THE FACULTY OF
UNIVERSITY OF MINNESOTA
BY

MICHAEL R. BURCUSA

IN PARTIAL FULFILLMENT OF THE REQUIREMENTS
FOR THE DEGREE OF
MASTER OF SCIENCE

RAJ SURYANARAYANAN
(ADVISER)

JUNE, 2013

Acknowledgements

I would like to acknowledge my immediate family, my advisor, Dr. Suryanarayanan, my master's committee for their immense aid in the completion of this thesis. I would also like to acknowledge the David J.W. Grant and Marilyn J. Grant Fellowship in Physical Pharmacy for financial support. Finally, I wish to acknowledge the American Association of Pharmaceutical Scientists (AAPS), the Advanced Photon Source (APS) at Argonne National Laboratory and the University of Minnesota Characterization Facility for the resources used in the completion of this work.

Dedication

This thesis is dedicated to my wonderful wife, Stephanie Larson Burcusa, Ph. D., L.P. and my beautiful daughter, Rose Mae Burcusa. These two individuals have suffered immensely (through my absence in the home, me being constantly distracted with school work and my infamous mood swings that have accompanied this work) over the years as I have pursued to advance my academic career. I apologize for these and hopefully will be a much better husband and father to you both in the immediate future.

Table of Contents

List of Figures

1.0 Introduction and theoretical background

1.1 Introduction

Pharmaceutical products are typically required to be stable, ideally at room temperature, for 18-24 months.(1, 2) Small molecules are usually formulated as tablets and capsules and consequentially will generally easily meet such shelf-life requirements. Large molecules such as monoclonal antibodies (mAb) have been approved for use in the treatment of diseases including cancer, rheumatoid arthritis and multiple sclerosis.(3) Since these macromolecules are unsuitable for oral administration they will invariably be administered parenterally.(4) Their poor solution stability necessitates formulation either as a frozen solution or as a freeze-dried (lyophilized) cake.(5)

Due to their complex structures, proteins and other macromolecules are inherently unstable. The mechanism of degradation is commonly through denaturation or agglomeration.(6-8) In addition to their inordinately large molecular weights, these pharmaceutical agents have multiple levels of structure ranging from the primary sequence of amino acids to the manner in which the polypeptide chain folds and combines with other chains leading to tertiary and quaternary structures.(9, 10) Destabilization of these proteins is manifested through loss of the native structure or conformation which can lead to a decrease of activity.(2, 11) In addition, mAbs are prone to agglomeration which may not necessarily inactivate the protein, but can lead to biocompatibility problems.(12) Research into the varied mechanisms of degradation and strategies to enhance the product stability is flourishing.

Due to stability issues, protein pharmaceuticals are often formulated either as frozen solutions or as freeze-dried powders.(13) Common to both frozen and freeze-dried formulations is the initial step of freezing an aqueous solution containing the protein as well as common excipients. The excipients' functions include: (*i*) control the pH, (*ii*) cause the reconstituted solution to be of physiological osmotic pressure, (*iii*) provide bulk and (*iv*) stabilize the protein during all of the processing steps and subsequent storage. If successful, the proper choice of excipients will lead to an FDA-approved product. Although water is by far the most common solvent used in frozen and freeze-dried formulations, it can induce instability in many proteins over pharmaceutically relevant timescales. Due to these instabilities, one of the overarching aims of each protein formulation is to minimize the water-protein interactions through removal (or phase separation) of free water.(14)

1.2 Motivation

Monoclonal antibodies are an important class of pharmaceuticals that have the potential to revolutionize the treatment of several diseases. In order to realize this success, however, all aspects of the production and delivery of these drugs must be well understood. A comprehensive understanding of the physiochemical properties of the liquid component of the frozen system (i.e. the freeze-concentrate) is required to enhance protein stability and to manufacture robust pharmaceutical products. In an effort to

progress the science of formulation development, this work investigates phase transitions of excipients in the freeze-concentrate.

1.3 Thesis overview

Development of robust protein formulations is of paramount importance to the pharmaceutical industry. Traditionally, the development of such products has been an empirical exercise. Efforts should be taken to transition lyophilization R&D away from an empirical exercise and towards an evidence-based science.

We begin the thesis with a review of phase transitions observed in a freeze-concentrate and the analytical techniques used to characterize these events. In Chapter 2, we present our research showing how buffer salts and amorphous sugars interact in the freeze-concentrate. We will show that these interactions may lead to heterogeneity in the freeze-concentrate as well as the formation of a molecular complex between dibasic phosphate and trehalose or sucrose. In the final chapter (Chapter 3) of the M.S. thesis, we explore the possibility of using xylitol, a 5-carbon sugar alcohol, as a lyoprotectant.

1.4 Frozen Protein Solutions

During the manufacture of freeze-dried and frozen dosage forms, the drug and excipients are dissolved in an aqueous medium and cooled under controlled conditions. The first thermal event to occur is usually ice crystallization, resulting in a dramatic increase in solute concentration.(4, 15) During the formation of this freeze-concentrate, many

undesirable, destabilizing events can occur which ultimately lead to drug degradation.(16)

The protein solution is cooled to the desired temperature at a controlled rate. At some point during cooling, ice will nucleate causing water to phase separate from the freeze-concentrate. During the formation of a freeze-concentrate, many stresses arise while others increase in magnitude - all of which may destabilize the protein. An example of a new stress is the origin of an ice-freeze-concentrate interface which is known to be an especially harsh environment and can lead to protein instability.(4) Other stresses such as the ionic strength of the buffer system increases in magnitude upon concentration. Together, these stresses cause the freezing stage to be an especially unforgiving one for labile proteins.(4)

Amorphous sugars are used as excipients due to their ability to protect the active protein in the freeze-concentrate.(17) By not crystallizing upon cooling, the sugar will become super-cooled. The properties of these sugars in the freeze-concentrate enable the sugar to intimately interact with and stabilize the protein. Upon further cooling, an aqueous sugar solution will undergo a phase transition to a glass at the glass transition temperature of the freeze-concentrate (T_g') – effectively diminishing the destabilizing forces in the freeze-concentrate. The term glass transition temperature and its abbreviation, T_g, represents the vitrification temperature of a pure substance. Angell defines the glass transition as the temperature corresponding to "the change in heat capacity which occurs

as the state of equilibrium is reestablished during warming after an initial cooling into the glassy state at a rate sufficiently high that no crystals have formed."(18)

If the product temperature is decreased below T_g', the freeze-concentrate will vitrify and "immobilize" the solutes. Most freeze-dried products are cooled well below their T_g' to prevent melt-back of the bulking agent during processing while most frozen protein products are stored at -20 °C - a temperature generally above the T_g' of pharmaceutical freeze-concentrates containing common cryoprotectants such as, sucrose and trehalose.

As opposed to freeze-dried products, frozen solutions are often used to store bulk material awaiting further processing.(19) The frozen products are generally stored in large walk-in freezers set at -20 °C until further processing. This bulk material is generally stored frozen in steel, plastic or Teflon containers ranging in size from 1 to 300 L. The solutions can be stored at these temperatures for up to three years.(20)

1.5 Freeze-Dried Formulations

The microenvironment experienced by the protein formulation during the initial stages of the freeze-drying process closely mimic that experienced during freezing of a frozen protein product. However, in most cases, the freeze-dried product is allowed to cool well below T_g' and thus the viscosity of the freeze-concentrate upon completion of the freezing stage will be orders of magnitude higher than at the storage temperature of frozen formulations (-20 °C).(21) Ice will always crystallize in a hexagonal packing form under pharmaceutically relevant conditions, but the size and shape (i.e. the morphology)

of ice crystals is dictated by the cooling rate.(15) A slower cooling rate leads to ice nucleation at high temperatures whereas a fast cooling rate leads to significant super-cooling before ice nucleation. Ice morphology can also be influenced by annealing above T_g', with longer annealing leading to larger ice crystals through Oswald ripening.(22) By controlling the size and shape of the ice crystals, one is able to control the size of the resulting pores which will have an influence on the kinetics of water removal; larger pores will lead to a more efficient sublimation process.(22) The drying process is initiated immediately after annealing.

During the drying step, vacuum is applied to the frozen product to facilitate ice sublimation. A typical vacuum in the freeze-dryer will be set to pressures of 50-150 mTorr.(23) The drying step is usually broken down to two separate sub-stages: primary and secondary drying. During primary drying, the temperature is set below the eutectic temperature (assuming the solutes have crystallized) to prevent melt-back, a process in which a fraction of the crystalline solute(s) has redissolved into the unfrozen water. Melt-back although not necessarily detrimental to the chemical stability of the product will lead to an inelegant cake with cracks, shrinkage or all-out loss of physical structure. The primary drying stage is designed to remove all of the *ice* from the product, while the *unfrozen* water in the freeze-concentrate remains. At the end of a typical primary drying cycle, up to 15-20% of the original water content remains.(15) During secondary drying, the temperature in the freeze-dryer is increased significantly so that the sorbed (liquid) water in the freeze-concentrate can be removed through evaporation. At the end of

secondary drying, the product (which will typically have less than 2% water) is brought to storage temperature and hermetically-sealed with a rubber stopper. The lyophile is reconstituted right before administration.

1.6 Frozen vs. freeze-dried formulations

When selecting the type of formulation to develop, the pharmaceutical scientist must weigh the benefits and disadvantages of each process. Freezing the product offers the most time- and cost-savings. However, the protein is subjected to a more stressful environment in the freeze-concentrate than in a dry environment. Additionally, due to challenges of maintaining the cold chain, bulk protein solutions are stored frozen (i.e. drug substance) while the individual dosage units (drug product) are prepared by freeze-drying.(15) Unfortunately, the freeze-drying process is extremely inefficient and difficult to scale. The scaling difficulties arise due to the manufacturing of freeze-dried products being a batch (as opposed to a continuous) process. Lyophilized products also are often stable at temperatures above 0 °C (either refrigerated or at ambient temperatures) and are thus more suitable for shipping and storage.

1.7 Excipients in formulations

Both frozen and lyophilized products require excipients to stabilize the pharmaceutically-active protein during ice freezing. Due to the pervasive presence of hydroxyl groups in carbohydrate structures, amorphous sugars are superior in their ability to form stabilizing interaction with both water and the protein through a vast network of hydrogen

bonding.(24) Timasheff and colleagues have used mathematical modeling to show that during freezing, these stabilizing sugars help maintain the native structure of the protein by forming a thin hydration shell of water around the protein. Cryoprotectants (amorphous sugars that protect a protein during freezing) are designed to be preferentially excluded from the surface of the protein which creates a local energy minimum state for the protein.(25)

In freeze-dried products, a stabilizer is often required to protect the protein both in the presence of ice and after the secondary drying. Sugars that are able to protect both during the freezing *and* the drying stages of lyophilization are referred to as lyoprotectants. To date, only two sugars are widely accepted as lyoprotectants by the freeze-drying community: trehalose and sucrose, both disaccharides (Figure 1.1). During the freezing stage, a lyoprotectant functions much like a cryoprotectant and must be preferentially excluded from the protein surface.(26) However, once the drying stage is initiated and the protective hydration shell is removed, the sugar must also be able to favorably interact with protein.(24) The accepted mechanism of lyoprotection during drying comes about from the water-replacement hypothesis.(27) Upon water removal, the sugar hydrogen bonds with the protein while similar bonds between water and the protein are disrupted. These hydrogen bonds maximize the energy required to denature the protein.(28) In addition, the lyoprotectant is required to remain amorphous throughout the process.(29) The glassy state is beneficial as it acts to physically hold the structure of the protein in its native form.(30)

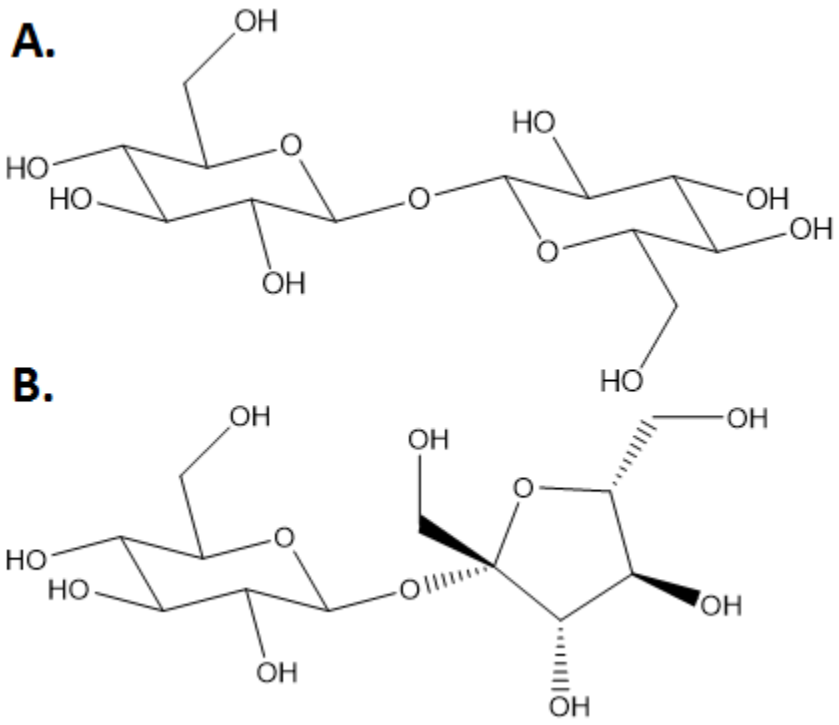

Figure 1.1 Chemical structure of trehalose (1A) and sucrose (1B).

In addition to amorphous sugars, a crystallizing solute is often included to serve as a bulking agent.(5) A bulking agent serves multiple functions in the freeze-dried formulation. When the bulking agent crystallizes from the freeze-concentrate, it will provide a physical scaffold for the other formulation ingredients. By serving as support, cake collapse, a phenomenon where the lyophile will crack, shrink and lose its elegant form, will be prevented. The bulking agent also serves to provide physical bulk to low-dose formulations. A bulking agent is also used by formulators to adjust the concentration of the reconstituted vial so that it is physiologically isoosmotic. Mannitol and glycine have both been used extensively by the pharmaceutical community as bulking agents.

Buffers are added to the formulation of both frozen and freeze-dried products so as to control the pH of the aqueous environment.(1) Although buffers work well in dilute solutions, they tend to crystallize in the freeze-concentrate when the solutions are super-saturated. The crystallization of a single buffer component will cause pH shifts which can lead to protein degradation.(31) Van den Berg and colleagues have demonstrated that upon freezing of a sodium phosphate buffered solution, a pH shift in the acidic direction will occur when the basic buffer component crystallizes as the dodecahydrate ($Na_2HPO_4 \cdot 12H_2O$) while the NaH_2PO_4 component remains in solution.(32)

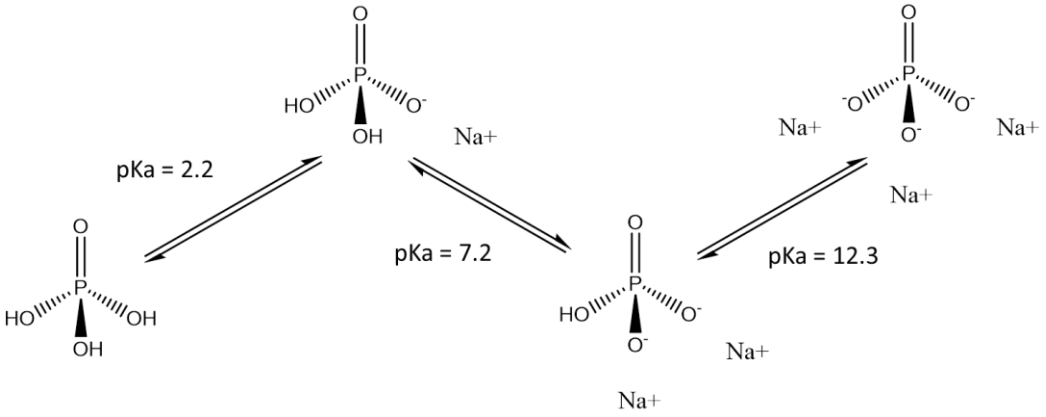

Figure 1.2 Ionization states and pK_a values of sodium phosphate. A sodium phosphate-buffered solution will generally exploit the second ionization state (pK_a = 7.2) as the pK_a is very close to physiological pH. The pH should be within a pH unit of the pK_a to have optimal buffer capacity.

Phosphate buffers have been extensively investigated due to their prevalent use in pharmaceutical as well as biopreservation industries (Figure 1.2). This buffer system was studied by van den Berg et al. in the 1950s (32, 33), Franks et al. in the 1970s and 1980s (34, 35) and in the 1990s by Rodriguez-Hornedo et al. (36, 37). Van den Berg's pioneering research into sodium phosphate employed an elegant method of determining

the eutectic points of both sodium and potassium phosphate salts under equilibrium conditions. While cooling aqueous solutions of sodium and potassium phosphate buffers, equilibrium was maintained by continuously seeding the solution with ice and the respective crystalline buffer components. The researchers sampled aliquots of the freeze-concentrate at specific temperature increments during freezing. Upon warming to room temperature, the pH values were determined. Using these measurements, along with the Henderson-Hasselbalch equation (Equation 1.1) (38, 39), the ratio of phosphate buffer components in solution was determined.

$$pH = pK_a + \log\frac{[A^-]}{[HA]} \quad \text{Equation (1.1)}$$

The experimental approach employed by van den Berg and his colleagues enabled them to document the events occurring throughout the freezing process under equilibrium conditions (Figure 1.3). From this figure, one can determine the final pH of an equilibrated freeze-concentrate adjusting for temperature and initial pH. For instance, a 1 M solution of Na_2HPO_4 will be at pH 9 (Figure 1.3, point C) at 0 °C. Upon initial cooling, the solution will become slightly more acidic until its eutectic point (Figure 1.3, point D). At the eutectic point, Na_2HPO_4 will crystallize as the dodecahydrate. Once the Na_2HPO_4 crystallizes, the freeze-concentrate will become more acidic and follow curve DE until the eutectic point of NaH_2PO_4 (Figure 1.3, point E). Upon complete equilibrium cooling to -9.9 °C, the pH will be ~3.6. Unfortunately, since systems of pharmaceutical interest are almost always frozen under non-equilibrium conditions,(34) it remained

essential that the pharmaceutical community find ways to explore freezing solutions under real, non-equilibrium conditions.

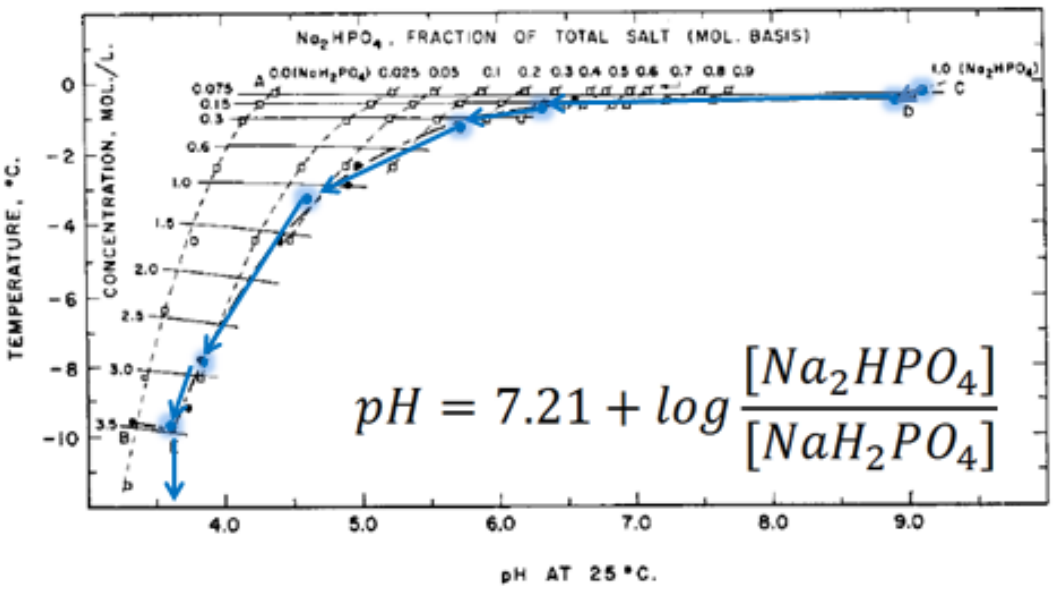

Figure 1.3 The effect of freezing on pH and composition of solutions of mono- and disodium phosphate.(32) Curve A-B: We are starting with a 0.075 M NaH_2PO_4 solution pH = 4 at 0 °C. Upon equilibrium cooling, ice crystallizes, the solute concentration increases to 3.5 M while the pH decreases to ~3.3 at ~-9.7 °C. Curves B-E: NaH_2PO_4 crystallizes, increasing the pH to ~3.6 at the eutectic point (E) wherein ice and NaH_2PO_4 simultaneously crystallize at -9.9 °C. Curve C-D is analogous to A-B wherein we start with a 0.075 M Na_2HPO_4 solution. Curve D-E is analogous to B-E in the same manner.

Murase and Franks used differential scanning calorimetry (DSC) to characterize sodium and potassium phosphate buffer systems, under non-equilibrium conditions.(34) However, they were hampered by issues such as the pronounced overlap of eutectic and ice melting endotherms. One of their lasting observations though was that the monosodium dihydrogen phosphate never crystallized and instead vitrified. This assertion was later supported by Chang and Randall who were able to detect a T_g' at -45 °C, attributed to freeze-concentrate containing NaH_2PO_4.(35)

The work of Chang and Randall also suggests that in the presence of some sugars, crystallization of Na_2HPO_4 was inhibited in formulations at sugar concentrations ≥ 10%.(35) Interestingly, they also stated that the vitrification of buffer salts will not lead to changes in pH of the freeze-concentrate, though no experimental evidence was provided in support of this assertion.

Recently, Rodriguez-Hornedo's group at the University of Michigan, utilizing a low-temperature pH probe, began to evaluate the change in pH resulting from the freezing of sodium phosphate and potassium phosphate buffered solutions.(36, 37) This work has recently been replicated by Kohle et al.(31) The low-temperature probe was made possible with two key alterations to the traditional pH probe: (*i*) utilizing a highly conductive glass membrane to allow faster exchange of ions and (*ii*) the development of an electrolyte solution containing glycerol so that the ion exchange across the membrane is not slowed by the freezing of the electrolyte solution (Figure 1.4).(40) The results of

these experiments confirmed that the freezing of a sodium phosphate buffer solution results in a pH drop attributable to crystallization of $Na_2HPO_4 \cdot 12H_2O$.(36, 41) Interestingly, freezing of potassium phosphate buffered solutions resulted in a pH increase from the crystallization of the monopotassium dihydrogen phosphate (KH_2PO_4).(37)

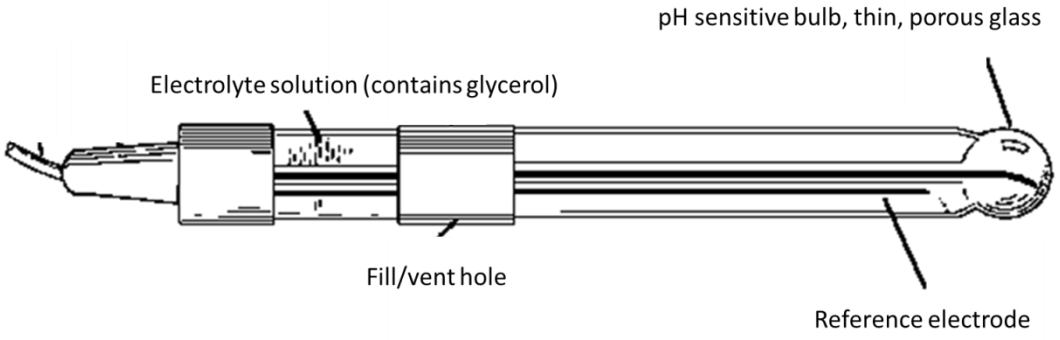

Figure 1.4 Low-temperature pH probe; reproduced from http://www.ph.co.za/probe.gif

Pikal-Cleland et al. demonstrated that pH shifts in frozen sodium phosphate buffers causes a loss in activity of tetrameric β-galactosidase, a pH sensitive protein.(42) Meanwhile Szkudlarek et al. showed that pH shift upon freezing of a potassium phosphate buffered solution causes degradation of the protein, lactate dehydrogenase.(37) In Pikal-Cleland's experiments, a single freeze-thaw cycle of a sodium phosphate-buffered system caused a change in pH from 7.0 to 3.8 and a 60% loss in β-galactosidase activity. In the presence of potassium phosphate, a much smaller pH change (7.0 to 7.3) resulted in a less pronounced loss in activity of lactate dehydrogenase (5-30%; dependent on initial buffer concentration).

More recently, Sundaramurthi et al. demonstrated a “pH swing” when sodium succinate buffer solutions were cooled. The researchers defined “pH- wing” as a phenomenon in which the pH would shift in one direction followed by the subsequent shift in the opposite direction; a pH swing is caused by the sequential crystallization of one buffer component followed by the crystallization of the other buffer component. The pH swing in a frozen sodium succinate buffered solutions was attributed to the sequential crystallization of first the acidic buffer salt (resulting in an increase in pH) followed by the basic buffer salt (resulting in a decrease in pH).(43) This observation was first made using a low-temperature pH electrode and was later corroborated with direct X-ray evidence of buffer salt crystallization using synchrotron radiation (Advanced Photon Source).

Using a laboratory X-ray diffractometer, it is possible to detect crystallization from aqueous solutions as long as the solute concentration is high (≥ 200 mM).(44) However, these concentrations are often well above those considered relevant to the pharmaceutical industry, and therefore in order to make observations that are directly applicable to the pharmaceutical industry, it is necessary that these systems are evaluated with a more sensitive technique such as synchrotron X-ray diffractometry (SXRD). SXRD has been demonstrated to detect crystallization from a 1 mM phosphate buffer solutions cooled to –50 °C (45). Varshney et al. have also demonstrated the utility of SXRD by

characterizing the different forms of glycine (salt and polymorphs) that crystallize under various processing conditions.(45-47)

1.8 Analytical techniques

1.8.1 Differential Scanning Calorimetry

The freezing of a pharmaceutical formulation generally causes one or more of the excipients to become super-saturated leading to a situation where they can either crystallize or vitrify with further cooling. In order to understand these concepts, it is useful to think of a one component system such as that of a molten chemical. Upon cooling a molten substance, it is thermodynamically favorable for that substance to crystallize at its freezing temperature. However, for many chemicals, including all cryo- and lyoprotectants such as sucrose and trehalose, crystallization does not occur because the time required for nucleation far exceeds timescales that are commonly used in the freeze-drying process. In these instances, the kinetics of crystallization dominate over the thermodynamics, and the substance will become super-cooled (Figure 1.5). The crystallization process can be broken down into two distinct processes: nucleation and growth. The nucleation of a crystal involves a critical size organizing in an ordered matrix. Once formed, crystal growth occurs by addition of molecules to the surface of the nuclei. Since nucleation is the limiting kinetic factor, crystallization rate and nucleation rate are often interchangeable. Equation 1.2 shows that nucleation rate (J) is inversely proportional to temperature (T);

$$J = A' \, exp\left[-\frac{16\pi\gamma^3 v^2}{3k^3T^3(\ln S)^2} + \frac{\Delta G'}{kT}\right] \qquad \text{Equation (1.2)}$$

where, A’ = experimentally determined constant, γ = interfacial tension, ν = molecular volume, ΔG’ = activation energy for molecular motion across the matrix (from crystal

seed to bulk), k = Boltzmann constant, S = degree of supersaturation. This equation demonstrates how further cooling will increase the viscosity of the freeze-concentrate leading to a decrease in the likelihood (or rate) of primary nucleation.(48) At a certain temperature, which depends on the rate of cooling but for strong glasses is typically around 2/3 of the freezing point on the Kelvin scale,(49) the substance will undergo a transition from a supercooled liquid to a glass. Upon vitrification, the mobility of the substance abruptly decreases by orders of magnitude causing the substance to appear and behave like a "solid". At the glass transition, properties such as viscosity, mechanical strength, enthalpy, and volume all change in a measurable manner.(50) Although the physical properties of the substance suggests that it is a solid, it lacks the long-range lattice order found in crystalline materials.(49, 51) The glass transition is a reversible process and is often measured upon warming.

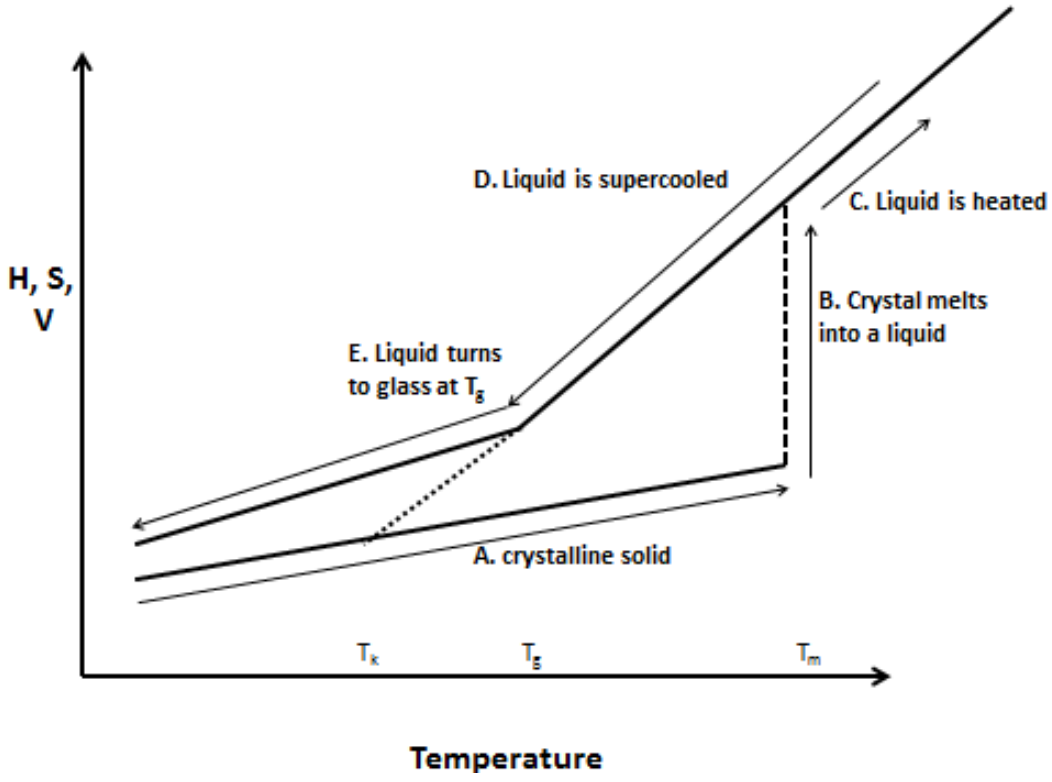

Figure 1.5 Relationship between temperature and enthalpy, entropy, or volume upon phase transitions. (A) A crystalline solid is warmed to its melting point (B) and the liquid is further warmed (C). Upon cooling of the liquid, crystallization does not occur and the liquid becomes supercooled (D). (E) At T_g, the liquid undergoes a phase transition to a glass. T_g depends on cooling rate where a slower cooling will result in an decrease in T_g. If the material was cooled infinitely slowly, the T_g may approach the Kauzmann temperature (T_k).

Differential scanning calorimetry (DSC) is one of the most widely used methods to characterize the glass transition. The freeze-concentrate will always include water and at least one solute and therefore be characterized by a T_g'. A sucrose-water freeze-concentrate has a T_g' of -47 °C(52) while a trehalose-water freeze-concentrate has a T_g'

of -35 °C.(53) For binary mixtures, the Gordon-Taylor equation (Equation 1.3) is used to calculate the glass transition temperature of a mixture of two components from the molar concentrations of each component in the mixture and the glass transitions of the pure components.(54)

$$T'_g = \frac{w_1 T_{g_1} + k w_2 T_{g_2}}{w_1 + k w_2} \qquad \text{Equation (1.3)}$$

Water has a T_g value of 136 K(55) and is considered a ubiquitous plasticizer.(56) As a plasticizer, when mixed with another glass-forming component, water will decrease the T_g of the solute. Most sugars of interest to the pharmaceutical community have known T_g values. These temperatures along with other valuable thermodynamic information can be found on a state diagram (Figure 1.6). When the concentration of water linearly influences the glass transition temperature of a substance, the mixture is termed a strong glass-forming supercooled liquid. On the other hand, a non-Arrhenius relationship is the hallmark of a fragile glass-forming supercooled liquid. Depending on the type of glass formed, the viscosity will have a linear (strong glass) or non-linear (fragile glass) dependence on temperature.

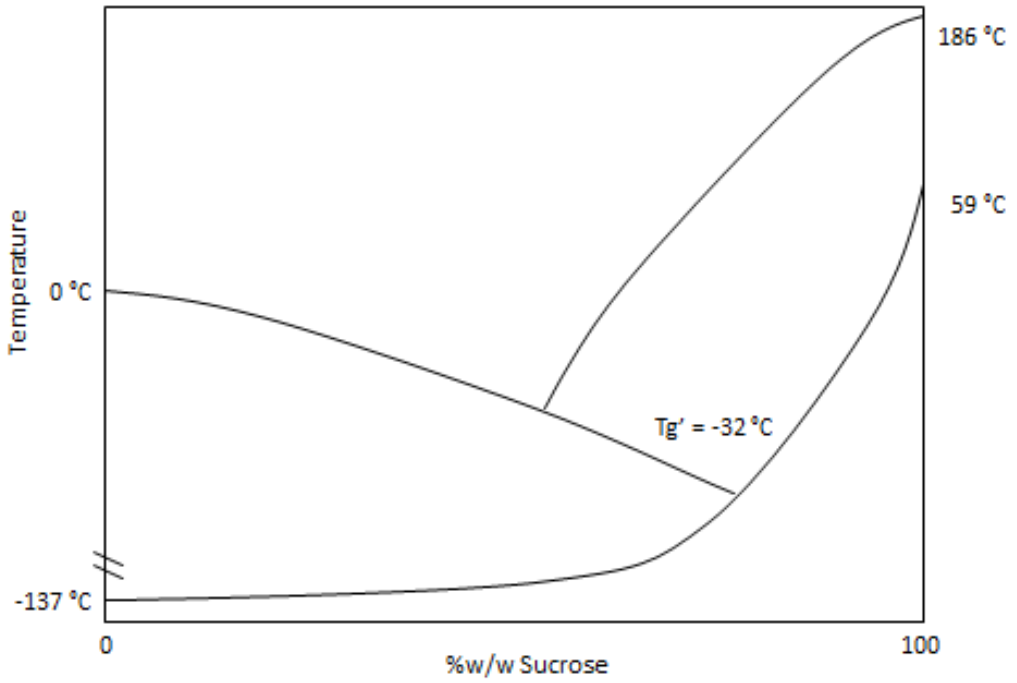

Figure 1.6 Schematic state diagram of sucrose-water system.

DSC has been extensively used to characterize freeze-concentrates.(57) DSC operates by continuously monitoring the heat capacity of the sample while the sample is subjected to controlled temperature program.(58) When the sample undergoes a change of state such as freezing, heat is released (enthalpy of freezing) and a peak is observed in the DSC curve. A glass transition event, on the other hand, is not characterized by a peak, rather the overall heat capacity of the sample changes resulting in a step change in heat capacity at the glass transition (Figure 1.7). From the results of a typical DSC experiment, researchers are able to obtain information about the temperature of a transition and the transition enthalpy. In addition to glass transitions, solute crystallization, melting and freezing are all phase transitions that can be characterized in a typical DSC experiment.

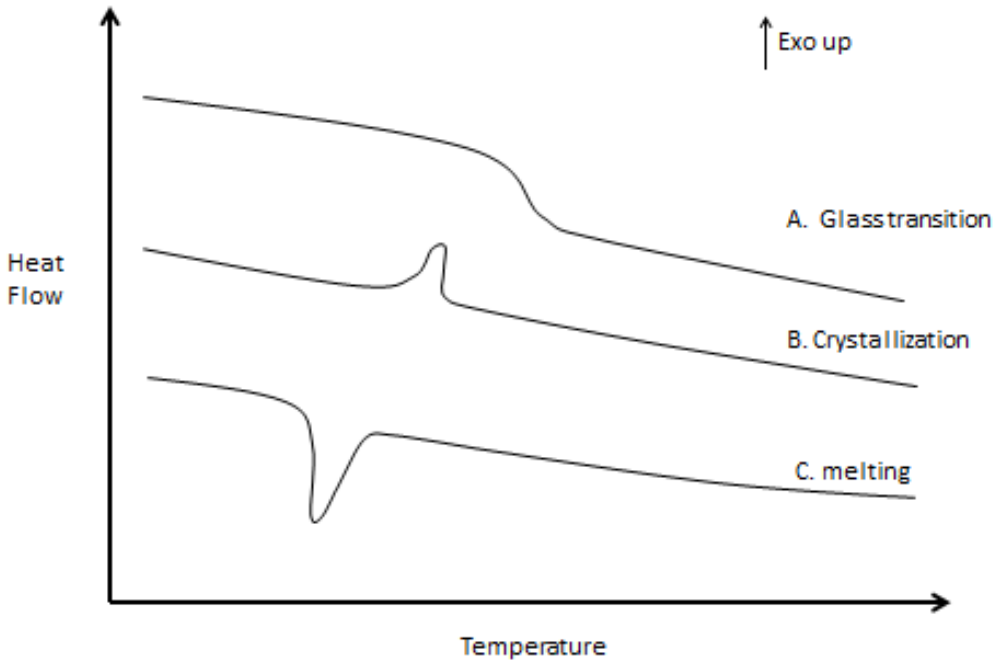

Figure 1.7 Schematic DSC curves of common phase transitions.

Modulated DSC (MDSC) is an advanced form of DSC where the temperature program is not applied in a linear fashion but in a sinusoidal manner. This enables one to differentiate between reversible and non-reversible thermal events. Since there is often an overlap of reversible and non-reversible transitions (for example glass transition accompanied by enthalpic recovery), modulation allows a researcher not only to separate these transitions but also determine the true transition enthalpies.

When utilizing DSC to characterize the thermal events in a typical freeze-drying run, the initial sample is generally an aqueous solution at room temperature. The sample will be subjected to a similar program as what is used in the freeze-dryer: typically cooling to a very low temperature (~ -50 °C) at 0.1 – 5.0 °C/min. When the sample is cooled, typically the first thermal event that will be observed is the freezing of water as an exothermic peak in the DSC; the corresponding release of heat of crystallization can be determined by integrating the area under the peak. Upon ice crystallization, a freeze-concentrate is formed. If one of the solutes were to crystallize, theoretically, one should observe a small exothermic peak (crystallization enthalpy). Unfortunately, when the solutes are at pharmaceutically relevant concentrations (~10 – 50 mM for a buffer) DSC is not sensitive enough to detect solute crystallization. Therefore, when conducting DSC studies, it is often necessary to increase the solute concentration in the samples. Upon further cooling, if there is an amorphous component such as trehalose or sucrose, one will observe the glass transition of the freeze-concentrate (T_g'). In addition to the temperature of the glass transition, one will also be able to determine the change in heat capacity at the transition (ΔC_p).

The information collected from DSC experiments is extremely useful in guiding the development of a lyophilization cycle. For instance, one should always conduct primary drying below the T_g' of the freeze-concentrate to prevent cake collapse. In addition, crystallization exotherms may be a reason for concern if the crystallizing solute was meant to remain in solution; this is the case when there is selective crystallization of a

buffer component. Other solutes, such as bulking agents are designed to crystallize during the freezing cycle. In order to fully evaluate the lyophilization run, other analytical techniques such as Fourier transform infrared spectroscopy (FTIR), low-temperature pH measurements and X-ray diffractometry (XRD) are required.

1.8.2 Fourier-Transform Infrared Spectroscopy

Organic molecules are able to absorb infrared radiation in the range from 10,000 to 100 cm^{-1} and convert this energy into molecular vibrations. Through the use of an infrared detector, one is able to glean valuable information about the molecule in question from the wavelength and intensity of various vibrational absorption bands which will appear as peaks in the interferogram. A typical Fourier transform infrared (FTIR) spectrophotometer tracks infrared (IR) vibrational-rotational bands in the mid-IR frequency range (4000 – 400 cm^{-1}). The precise frequency of these IR bands is dependent on the type of bond (single, double, triple, aromatic, etc.), the length of the bond and the mass of the atoms which are connected by the molecular bond. As a general rule, the stronger the chemical bond, the higher the frequency of vibrations.(59)

FTIR is only able to detect molecular vibrations that affect the dipole of a molecule. These vibrations must be asymmetric in order to change the dipole moment. The typical molecular vibrations of interest are stretching and bending vibrations. A stretching vibration refers to vibrations along the molecular bond as the bond length changes in a rhythmic manner. A bending vibration on the other hand will result from a change in the

bond angle and therefore only arise from strings of 3 consecutive atoms (X-A-Y) where the bond angle XAY will rhythmically change from smaller to larger angles.

In a planar molecule such as CO_2, there are theoretically (3N – 5) vibrations where N is the number of atoms in the molecule. A non-planar molecule (which is typical for most pharmaceutically active materials as well as most formulation excipients) will have (3N – 6) vibrations. However, this theoretical number of vibrations is seldom found as there are many factors influencing the number of observed vibrations. For example, combination vibrations and overtones can arise under common experimental conditions resulting in an increased number of vibrations than are predicted by the above rule. Furthermore, other vibrations may either not be detectable or fall outside the working range of the FTIR instrument. Additionally, two vibrations overlapping in the IR spectrum will appear as one peak. Finally as noted earlier, since FTIR can only detect vibrations that cause a change to the dipole of the molecule, any vibrations that do not change the dipole are impossible to detect by FTIR.

Combination bands such as those that result from *both* stretching and bending come about from coupled interactions between these bands. Coupled interactions however do not translate over extended parts of the molecule and a vibration will not be coupled with another when they are separated by one or more carbon molecules.(59) Coupled interactions only arise from vibrations with the same symmetry and must involve common atoms; the absorptions of the individual bands must also be near the same

frequency in order for a coupled interaction to appear in the FTIR spectrum. For instance, coupling of bending and stretching vibrations will only be detected if the stretching bond forms one side of the changing angle.

1.8.2.1 Intermolecular interactions in FTIR

Many polar organic compounds are only soluble in solvents such as water. The presence of water will often result in hydrogen bonds between the water molecule and various functional groups in the solute molecule. These hydrogen bonds will affect the strength and frequency of the chemical shifts, as the bond energy is diminished in the presence of hydrogen bonding causing an increase (red shift) in wavelength which in turn lowers the frequency of the vibrational bands of the concerned functional groups.(60) One is also able to differentiate between hydrogen bonding in solution as opposed to crystalline material. Crystalline materials yield sharp peaks. In solution, the hydrogen bonds will vary in length and orientation as the solutes move about in the protic medium. Thus, in solution, there is peak broadening.(61)

In aqueous solutions, one is also able to glean valuable information from the H_2O scissoring mode peak (~1650 cm^{-1}). A red shift in this peak indicates hydrogen bonding between water and the solute.(61) Interestingly, the IR spectrum of amorphous trehalose closely resembles that of an aqueous trehalose solution. Wolkers et al. concluded that this indicates that the strength and direction of hydrogen bonding in amorphous trehalose (trehalose-trehalose interactions) is very similar to that between water and trehalose in the

aqueous solution.(61) This observation may shed light on why trehalose is an excellent lyoprotectant in that the interactions between trehalose and the protein in the dry state is very similar to the interactions between water and the protein in the liquid state.

The T_g of a substance (and thus T_g' of a mixture) can be determined experimentally with FTIR. By plotting the position of the -OH stretching vibration of a sugar against temperature, one will observe a linear change in the temperature dependence of the peak position up to the T_g. Figure 1.8 demonstrates that at T_g however, there will be a distinct change in the slope and above T_g, a new linear slope will be realized.(62)

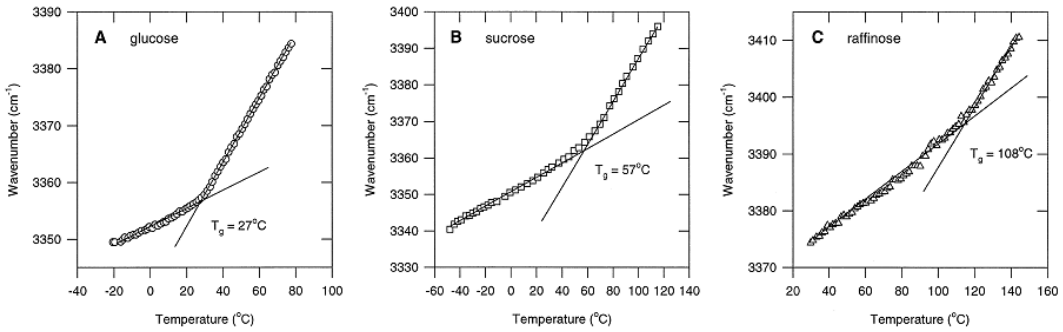

Figure 1.8 T_g can be determined by FTIR by identifying the break in the linear dependence of peak position on temperature.(62)

1.8.3 Low-Temperature pH Measurements

A change in pH of the freeze-concentrate can lead to protein degradation or agglomeration.(4, 11-13, 31, 37, 42) Therefore it is critical that development of new protein formulations which includes a freezing step incorporate low temperature pH measurements. In a typical measurement, a low temperature pH probe is placed in a

solution cooled at a controlled rate (Figure 1.9). The pH probe and a thermocouple are connected to an automated data collector. The pH probe is usually calibrated for variable temperature measurements with four different commercially available calibration buffers (pH = 2, 4, 7, 10) at different temperatures (typically, 0, 10 and 25 °C). The linear relationship between electromotive force (EMF) which is recorded by the pH probe and the medium pH is shown in Equation 1.4. The relevant slope and y-intercept of Equation 1.4 is then extrapolated to the temperature of measurement (≥ -25 °C).

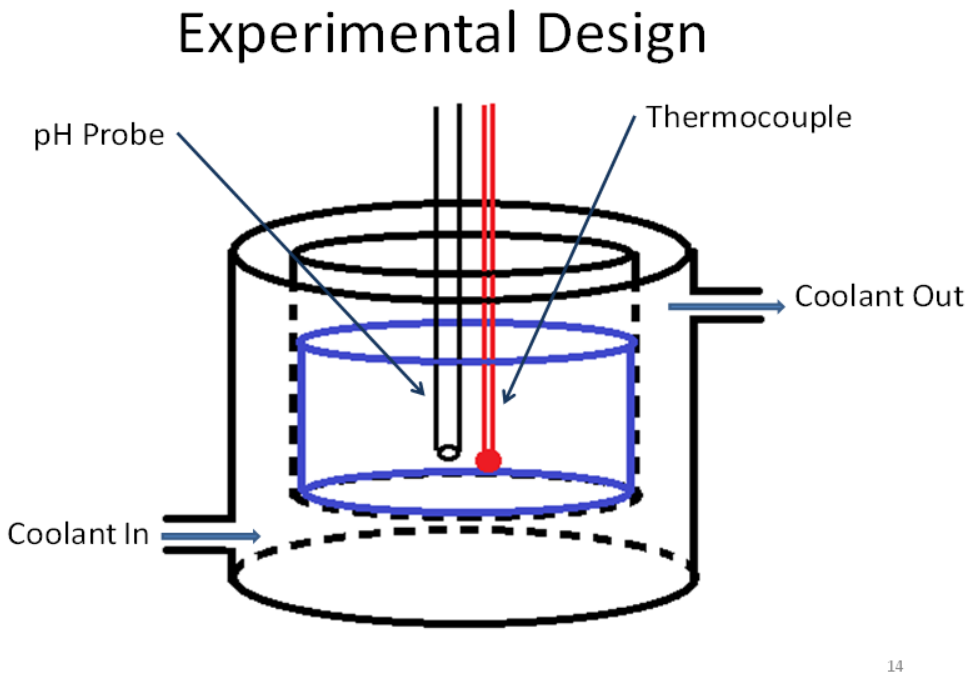

Figure 1.9 A typical set-up for a low temperature pH measurement. About 100 ml of the test solution is placed into a jacketed flask. The solution is cooled at a controlled rate by a circulating water bath while electrical potentials and solution temperature are measured continuously.

$$\mathrm{pH} = \left(\frac{m_1}{T} + m_2\right) \times \mathrm{EMF} + \left(\frac{b_1}{T} + b_2\right) \qquad \text{Equation (1.4)}$$

In Equation 1.4 m_1, m_2, b_1, b_2 are constants calculated from calibration with standard buffers and EMF is the electromotive potential (as recorded by pH probe).

1.8.4 X-ray diffractometry (XRD)

X-ray diffractometry (XRD) is also an immensely valuable technique for analysis of frozen solutions as well as final lyophiles. Lab source XRD equipment is widely available and relatively safe and easy to use.(63) X-rays are electromagnetic radiation with a wavelength about 1 Å (about the same size as an atom). The discovery of X-rays enabled scientists to probe crystalline structure at the atomic level.(64) Due to this characteristic wavelength, the X-rays are able to penetrate into a crystal and reflect off the regular crystalline planes at characteristic angles. The resulting pattern can be used to identify the crystalline components in the sample. In the analyses of frozen aqueous solutions, peaks from hexagonal ice will dominate and prevent the detection of other components in the ice peak region (triplet at ~22 – 26 °2θ; single peak at ~33 °2θ; using Cu Kα radiation). However, outside the angular range of ice peaks, other peaks from crystalline solutes can be used for identification purposes.

In a typical experiment, 500 µL – 1.0 ml of the formulation solution is added to a copper XRD holder and the solution is cooled at a controlled rate. Since ice is unique in that it expands upon freezing, the surface of the frozen mass will not be coplanar with the sample holder surface and without the use of a Göbel mirror, the crystalline peaks will be displaced slightly.(65) However, modern software is able to account for these displacements. The main limitation to XRD then is the limited sensitivity. To detect small amounts of a crystalline material in a heterogeneous matrix, it is often necessary to utilize more sensitive, but costly analytical measures such as synchrotron XRD (SXRD).

1.8.5 SXRD

Synchrotron X-rays are radiated from electrons as they approach the speed of light in a particle accelerator. Due to the costs and expertise required to maintain such capabilities, synchrotron sources are not widely available for commercial use. However, the U.S. government does support beamlines at Argonne National Laboratory and Brookhaven National Laboratory and access is available to those that successfully submit an application for its use. SXRD can detect crystalline components at very low concentrations. For instance, Varshney et al. used SXRD to detect $Na_2HPO_4 \cdot 12H_2O$ crystallization from 1 mM phosphate buffer solutions.(45)

In a typical synchrotron experiment, the test solution is placed in a sample holder and cooled at a controlled rate to the desired temperature. This is carried out in a water-bath outside the beamline. When an SXRD scan is required, the sample will be exposed to radiation for only a few seconds. The waves pass through the sample (transmission mode) and will diffract at signature angles. The diffracted rays are detected by a 2D detector and interpreted after integration (Figure 1.10).

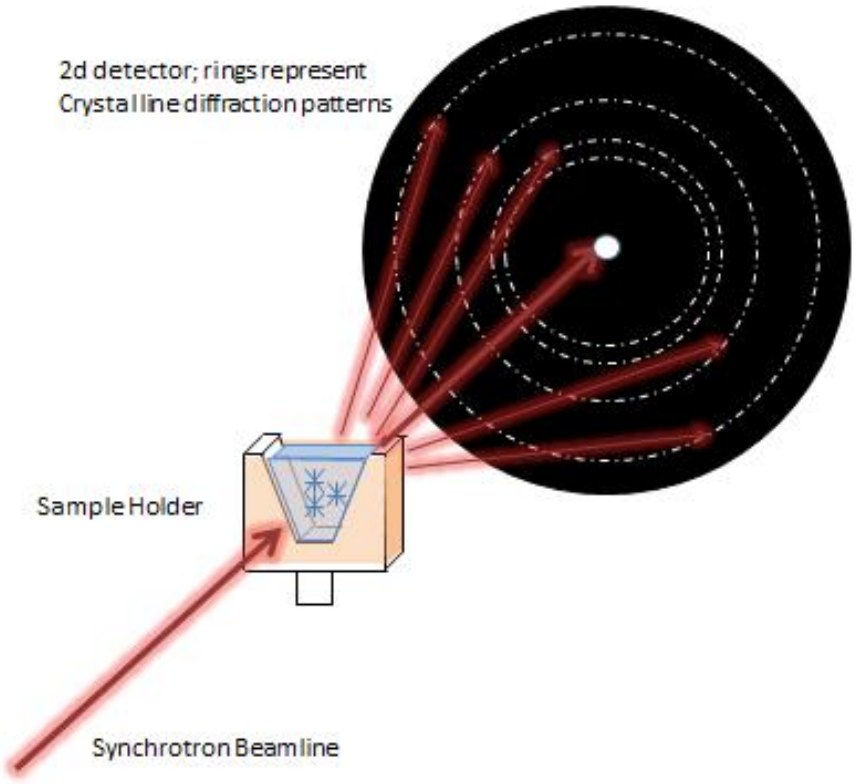

Figure 1.10 Schematic of the synchrotron XRD experiment.

1.9 Thesis Hypotheses

1.9.1 Chapter 2

The change in pH upon freezing of an aqueous buffered solution has been attributed in the literature to selective crystallization of a single buffer component while the other buffer component remains in solution. In our experiments however, we have found evidence of pH change *without* buffer salt crystallization. The objective of Chapter 2 is to elucidate the mechanism of pH change without buffer salt crystallization.

The working hypotheses of Chapter 2 are:

1. A shift in pH can occur in the freeze-concentrate without buffer salt crystallization and is attributed to complexation between the amorphous sugar and dibasic phosphate.
2. In frozen solutions, in the presence of amorphous sugars, the freeze-concentrate consists of "sugar-rich" and "water-rich" regions. The properties of these regions are dictated by all of the components in the region.

1.9.2 Chapter 3

Currently only two compounds are available for use as lyoprotectants. These two compounds, both disaccharides, are sucrose and trehalose. However, each of these sugars has documented deficiencies. The glycosidic linkage in sucrose will hydrolyze at low pH values, while trehalose tends to slowly crystallize upon annealing close to the T_g' of the freeze-concentrate. Furthermore, we have documented that a pH shift of at least 1.5 units will occur upon freezing a sodium phosphate buffered solution in the presence of either lyoprotectant. Xylitol, a 5-carbon sugar alcohol, has been identified as a possible lyoprotectant and merits characterization.

The working hypotheses of chapter 3 are:

1. Xylitol is more effective at preventing pH change in the freeze-concentrate than either trehalose or sucrose.
2. Xylitol is an effective lyoprotectant.

2.0 Interactions Between Sugars and Buffers in Frozen Solutions

2.1 Introduction

Large molecules such as proteins need to be formulated as solutions since they are invariably administered parenterally. However, poor solution stability often necessitates a final formulation either as a frozen solution or as a freeze-dried cake (5). In addition to the active ingredient, frozen and freeze-dried formulations often contain a disaccharide (sucrose or trehalose), and a buffer. These components, referred to as excipients, are added to maintain the stability of the active ingredient. Freeze-dried formulations are processed by first freezing the solution followed by drying under reduced pressure, whereas frozen formulations do not undergo the drying step. The design of the freeze-drying process has been extensively reviewed elsewhere (23, 66). The freezing stage, common to both freeze-dried and frozen formulations, is the focus of this work.

When a dilute aqueous solution is cooled, ice usually crystallizes first, resulting in the formation of a freeze-concentrate. Numerous factors, including the system composition and the processing conditions will dictate the behavior of the solutes in frozen solutions. The influence of processing conditions and formulation composition on the chemical stability of the active ingredient (typically a macromolecule) has been extensively investigated (4). However, it is increasingly recognized that the phase behavior of the excipients in the system will dictate the stability of the active ingredient (15). Therefore, it is imperative to comprehend the interplay of the formulation and processing factors. While drug-excipient interactions have been extensively investigated, little attention has been paid to excipient-excipient interactions. For example, since buffer and sugar

(protectant) are ubiquitous components of protein formulations, their potential interactions warrant consideration.

Sodium phosphate is a popular buffer choice in light of its long history of use in biological research. This buffer system was studied under equilibrium conditions by van den Berg and Rose. When phosphate buffer solution (pH 7.6 at room temperature) was frozen, crystallization of disodium hydrogen phosphate dodecahydrate ($Na_2HPO_4 \cdot 12H_2O$) caused a pronounced shift in the freeze-concentrate pH to 3.6 (32). The consequence of such a pH change on protein stability was demonstrated by Pikal-Cleland et al. In their system, a pH shift from 7.0 to 3.8 resulted in a 60% loss in β-galactosidase activity (42).

While van den Berg and Rose conducted their experiments under equilibrium conditions (by appropriately seeding the frozen solutions), the more recent studies were all under non-equilibrium conditions.(34, 36, 67) These studies are more relevant to processing and manufacture of biologics and pharmaceuticals. The culmination of the numerous investigations, under both equilibrium and non-equilibrium conditions, is that the observed pH shifts are attributable to the selective crystallization of $Na_2HPO_4 \cdot 12H_2O$. X-ray diffractometry (XRD) of frozen solutions is a powerful and unambiguous method to detect crystallization of buffer components (68). The use of synchrotron radiation has resulted in substantial enhancement in sensitivity and detection of buffer salt crystallization even from dilute (1 mM initial concentration) buffer solutions (45).

One possible approach to prevent buffer salt crystallization is the addition of non-crystallizing solutes such as sugars. This was demonstrated in succinate buffer systems which exhibit a very pronounced tendency to crystallize when cooled (69). However, we have recently observed a pronounced pH shift when phosphate buffered sugar (sucrose or trehalose) solutions were frozen. Interestingly, in these systems, there was no indication of buffer salt crystallization even with the use of synchrotron radiation (70). Therefore the overall goal of our work was to understand the mechanism of this pH shift in the absence of buffer salt crystallization.

Disaccharides such as trehalose and sucrose are widely used in frozen and freeze-dried formulations due to their ability to remain amorphous and to form stabilizing interactions with the dissolved proteins. Upon cooling an aqueous sugar solution, it will undergo a transition from the rubbery to the glassy state at its glass transition temperature. Interestingly, trehalose and sucrose exhibit two glass transition temperatures - evidence of two "populations" in the freeze-concentrate (71-73). The lower and higher temperature glass transitions are referred to as T_g" and T_g' respectively. The reported T_g' and T_g" of sucrose are -33.3 °C and -41.5 °C respectively, while those of trehalose are -30.2 °C and -37.4 °C (74). The existence of two freeze-concentrate populations raises some interesting questions. (*i*) What is the difference in solute composition(s) between the two populations? (*ii*) More importantly, how do we ensure effective stabilization of the active ingredient in each of these environments? In an effort to answer the first question, we

investigated the freeze-concentrate compositions in our model systems which consisted of a buffer (sodium or potassium phosphate), a disaccharide (sucrose or trehalose) and water. The second question was outside the scope of our current investigation.

Trehalose is a popular and effective stabilizer of biologics (including proteins) and has been well studied. The stabilizing effect of trehalose was substantially enhanced in the presence of borax (75, 76). This was attributed to the formation of a trehalose-borate (1:1) complex in the freeze-concentrate. Interestingly, the interaction of trehalose with boric acid also caused a pronounced change in the apparent pK_a of boric acid (77, 78). The T_g' of the complex was much higher than that of trehalose, attributed to decreased mobility. As a result, the complex was a more effective lyoprotectant than trehalose alone (75, 76). However, due to toxicity concerns, the use of boric acid is restricted to topical pharmaceutical formulations.

Phosphoric acid buffers, in light of their structural similarity to boric acid, are also believed to form a complex with trehalose (79). However, this conclusion was based on the investigation of freeze-dried systems. Our interest is to explore complex formation in frozen systems. This would help us explain the observed pH shifts *in the absence of buffer crystallization*. The objective of this work is to understand how each buffer salt (NaH_2PO_4 and Na_2HPO_4) interacts with the sugar in the freeze-concentrate. Therefore, we will: (*i*) document the pH shift in frozen buffer (sodium phosphate) – sugar (sucrose or trehalose) systems at different buffer and sugar concentrations, (*ii*) evaluate solute

crystallization in these frozen systems using synchrotron radiation, (*iii*) investigate the thermal behavior (glass transitions) by differential scanning calorimetry with the goal of identifying the two freeze-concentrate populations and, (*iv*) use IR spectroscopy to characterize the two populations and specifically the complexation between trehalose and the buffer components in the two populations.

By developing a comprehensive understanding of this pharmaceutically relevant system, we hope to guide the formulator in making a rational selection of formulation components. This is an excellent example of an excipient-excipient interaction facilitating the design of a robust freeze-dried formulation.

2.2 Materials and Methods

Monosodium dihydrogen phosphate monohydrate ($NaH_2PO_4 \cdot H_2O$), disodium hydrogen phosphate, trehalose dihydrate ($C_{12}H_{22}O_{11} \cdot 2H_2O$), (all from Sigma) sucrose, sodium hydroxide, potassium hydroxide (Mallinckrodt) and potassium dihydrogen phosphate (J.T. Baker) were purchased with purity >99% and were used without further purification. Deionized water was degassed by holding at 70 °C for 5 min and membrane filtered (0.45 μm PTFE, Fisher). The degassed water, stored in a closed container at room temperature, was used to prepare buffer solutions within a week of preparation. A pH meter (Oakton), calibrated with standard buffer solutions (Oakton standard buffers; pH 2.00, 4.01, 7.00 and 10.00; certified by NIST) was used.

2.2.1 Preparation of Buffer Solutions

Solutions were prepared by dissolving the appropriate amount of disodium hydrogen phosphate (or dipotassium hydrogen phosphate) and sugar (sucrose or trehalose), then adjusting the pH with NaOH (for the sodium phosphate solutions) or KOH (for the potassium phosphate solutions) to the desired pH (± 0.1) at 25 °C. The final buffer concentration ranged between 5 and 500 mM. All the solutions were membrane filtered (0.45 μm, PTFE) and used immediately upon preparation.

2.2.2 Differential Scanning Calorimetry

A differential scanning calorimeter (DSC) (Q2000, TA instruments, New Castle, DE, USA) equipped with a refrigerated cooling accessory was used. The cell constant was

determined using indium and temperature calibration was performed using indium, tin and water as standards. The aluminum pan containing the solution was hermetically sealed. The samples were cooled from RT to -75 °C at 0.1 °C/min, held for 15 minutes and warmed to RT at 2 °C/min. All DSC measurements were done under dry nitrogen purge.

2.2.3 Synchrotron XRD (SXRD)

The experiments were performed at the synchrotron beam line (6-ID-B, Advanced Photon Source), Argonne National Laboratory (Argonne, IL, USA). The variable temperature stage (High-Tran Cooling System) was attached to the Eulerian cradle (Huber 512) using an aluminum (Al) plate. An X-ray beam (0.76534 Å; beam size 100 (vertical) × 200 (horizontal) μm) was used, wherein the flux of the incident X-rays (intensity: 1,013 photons/s/mrad^2/mm^2) was attenuated to prevent detector saturation. The monochromator used was triple-bounce, channel-cut, [111] faces of a polished Si single crystal and limited the line broadening to its theoretical low limit, i.e. the Darwin width. An image plate detector (Mar345) with 3,450 × 3,450 pixel resolution in 34.5 mm diameter area, with a readout time of 108 seconds (best resolution mode), was used. The sample to detector distance was set to 500.1 mm. The calibration was performed using a silicon standard (SRM 640b, NIST). The experimental setup was described in detail earlier (46).

2.2.4 Fourier Transform Infrared Spectroscopy

In a typical experiment, 100 nL of the experimental solution was deposited between two CaF_2 windows. The windows were 16 mm in diameter and 0.5 mm in thickness. The windows were sealed with vacuum grease to eliminate evaporation and to generate a thin uniform film, ~ 1 μm thick. The sealed sample was then transferred to a Fourier transform infrared spectrometer (FTIR: Thermo-Nicolet Continuum equipped with a Mercury Cadmium Telluride detector, Thermo Electron, Waltham, MA) equipped with a FDCS 196 (Linkam Scientific Instruments Ltd., UK) freeze-drying cryostage. The FTIR sampling resolution was 4 cm^{-1}, and 128 IR scans were averaged per spectra in the 9000-900 cm^{-1} wavenumber range. A cryo-stage was used for precise control of the sample temperature. The sample was cooled to -100 °C at 2 °C/min and heated back to the room temperature at 0.5 °C/min. The IR spectra were analyzed using Omnic (Thermo-Nicolet) and Peakfit4 software (Systat Software, Inc., San Jose, CA).

2.2.5 Low Temperature pH Measurements

About 100 ml of solution was placed in a jacketed beaker (250 ml) connected to a water bath with an external controller unit (Neslab RTE 740, Thermo electron, NH). A low-temperature pH electrode (Inlab® cool, Mettler Toledo, Switzerland) was placed in the center of the sample and connected to a pH meter (pH 500 series, Oakton, Singapore) to monitor the electromotive force (EMF), from which the pH of the solution was calculated. Initially, the solutions were allowed to equilibrate at 0 °C, and then cooled to −25 °C at 0.5 °C/min and held at -25 °C for at least 3 hours.

The change in pK_a of the phosphate buffer as a function of temperature was determined using the Nernst equation, where E = potential difference between sample and reference electrode, E_0 = standard potential of the electrode at a_{H^+} = 1 M, R = gas constant, T = temperature (K), n = valency of ion, F = Faraday constant (Equation 2.1).

$$E = E_0 - 2.3\frac{RT}{nF}log(a_{H^+}) \qquad Equation\ (2.1)$$

2.3 Results

In frozen systems, the selective crystallization of a buffer component is known to cause a pH shift, which can be pronounced (32). Since this pH change has the potential to be detrimental to protein stability, efforts should be made to minimize such pH deviations (4, 37, 67). This paper aims to evaluate how a lyoprotectant influences the properties of the buffer. In an effort to better characterize the interactions between an amorphous sugar and an inorganic buffer, frozen trehalose (or sucrose) solutions buffered with sodium (or potassium) phosphate will be characterized using thermoanalytical, spectroscopic and diffractometric techniques.

2.3.1 SXRD of frozen buffer solutions

SXRD studies of buffer solution revealed selective crystallization of the dibasic salt as a dodecahydrate ($Na_2HPO_4 \cdot 12H_2O$) which was responsible for the observed pH shift (Figure 2.1, upper-right quadrant). Trehalose (240 mM) effectively inhibited buffer salt crystallization and this effect persisted even after annealing for 33 hours at –25 °C (Figure 2.1).

In order to determine the inhibitory effect of trehalose, solutions with different ratios of buffer to trehalose were systematically investigated by SXRD (panels a to f; Figure 2.2). In the absence of trehalose, the buffer salt crystallized readily (panels a and d; Figure 2.2). When the molar concentration ratio of sugar to buffer was > 1, there was no evidence of buffer salt crystallization (panels c, e and f; Figure 2.2). However, when this

ratio was < 1, crystallization of $Na_2HPO_4 \cdot 12H_2O$ could be readily discerned (panel b; Figure 2.2). These results suggest that a 1:1 molar ratio of sugar to buffer is adequate to prevent buffer salt crystallization.

In contrast to the behavior of the sodium phosphate buffer systems, the pH of potassium phosphate buffered systems increased (Figure 2.3) due to the selective crystallization of KH_2PO_4 (32, 34). As before, trehalose completely inhibited the buffer salt crystallization when the concentration ratio of sugar to buffer was > 1 (data not shown). Since we are observing a pH change even when there is no evidence of buffer salt crystallization, we must consider that the observed pH shift through a different mechanism.

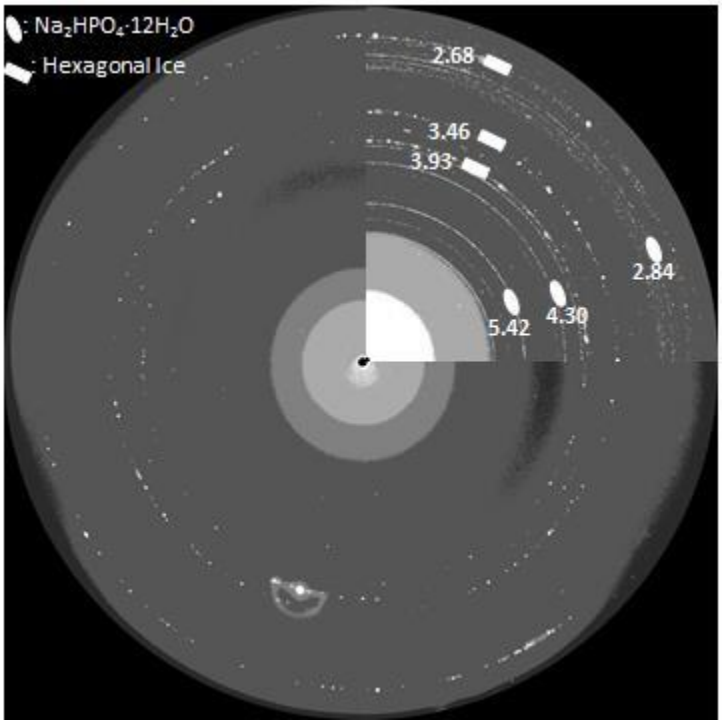

Figure 2.1 A 2D-SXRD image of a frozen aqueous solution containing sodium phosphate buffer (50 mM*) and trehalose (240 mM*). The solution was cooled from 25 to -25 °C at 0.5 °C/min, annealed

at -25 °C for 33 hours and the SXRD pattern was collected. An image from an identically treated 50 mM sodium phosphate solution without trehalose is overlaid in the top-right quadrant. The d-spacings (Å) of some characteristic lines of $Na_2HPO_4 \cdot 12H_20$ and ice are shown. *In this, as well as the subsequent figure, the initial solute concentrations (at RT) are provided.

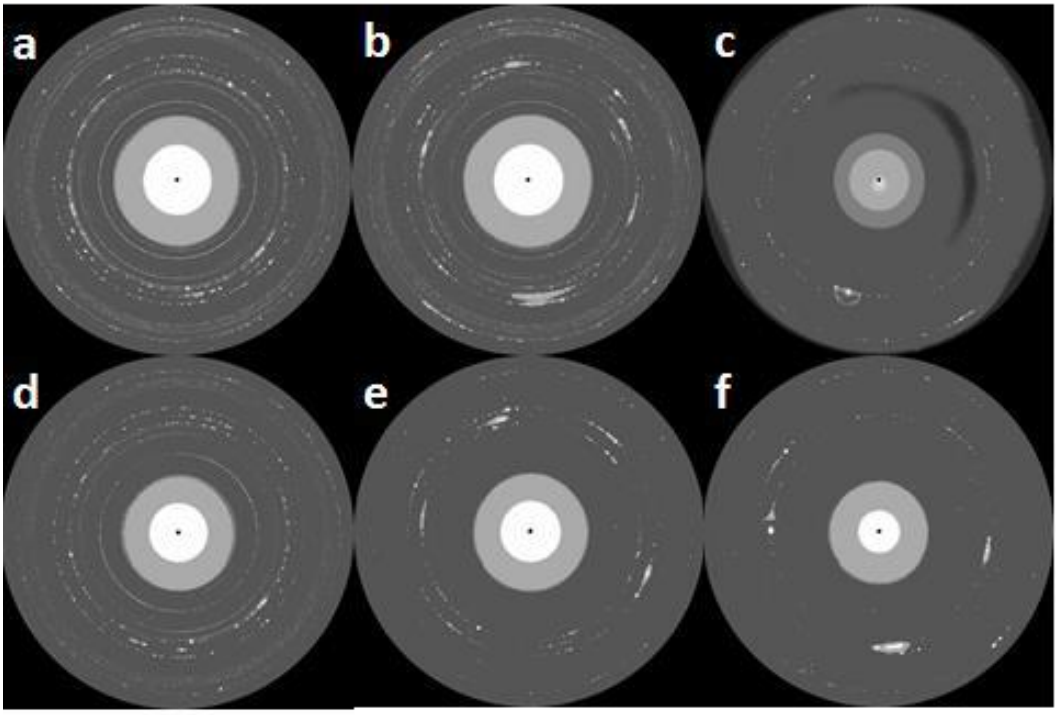

Figure 2.2 2D-SXRD images of sodium and potassium phosphate buffered solutions cooled from 25 °C to -25 °C at 0.5 °C/min. The patterns were collected at -25 °C after 24 hours of annealing. a. 100 mM sodium phosphate; b. 100 mM sodium phosphate, 80 mM trehalose; c. 100 mM sodium phosphate, 160 mM trehalose; d. 50 mM sodium phosphate; e. 50 mM sodium phosphate, 80 mM trehalose; f. 50 mM sodium phosphate, 160 mM trehalose.

2.3.2 pH shifts in frozen buffer solutions

A phosphate buffer solution (100 mM) when cooled from room temperature to -25 °C exhibited a pH shift of 2.1 units (Figure 2.3). This was caused by the crystallization of $Na_2HPO_4 \cdot 12H_2O$ (confirmed by SXRD; Figure 2.1). The presence of trehalose (or sucrose) attenuated the pH shift (Figure 2.3). Interestingly, there was no evidence of buffer salt crystallization when the frozen solutions were subjected to XRD using a laboratory source (data not shown). When the systems were subjected to SXRD, again there was no suggestion of buffer salt crystallization. As mentioned earlier, using SXRD, buffer salt crystallization was detected even from dilute (1 mM) buffer solutions.(45) In light of the extremely high sensitivity of SXRD, we conclude that the pH change is occurring *without* buffer salt crystallization.

Interestingly, at low sodium phosphate concentration (50 mM), both sucrose and trehalose, irrespective of concentration, had minimal influence on the observed pH shift (Figure 2.3). The pH decreased by 1.6 pH units in the absence of sugar, while the decrease was 1.1 – 1.4 pH units in the presence of sugar. In contrast, the pH of a potassium phosphate buffered solution *increased* by 0.9 pH units (i.e., became basic) upon freezing which is attributed to the selective crystallization of monopotassium phosphate (KH_2PO_4).(32). Interestingly, in the presence of sugar, the pH shift occurred in the *acidic* direction (Figure 3). SXRD however, demonstrates that the acidic shift cannot be attributed to buffer salt crystallization.

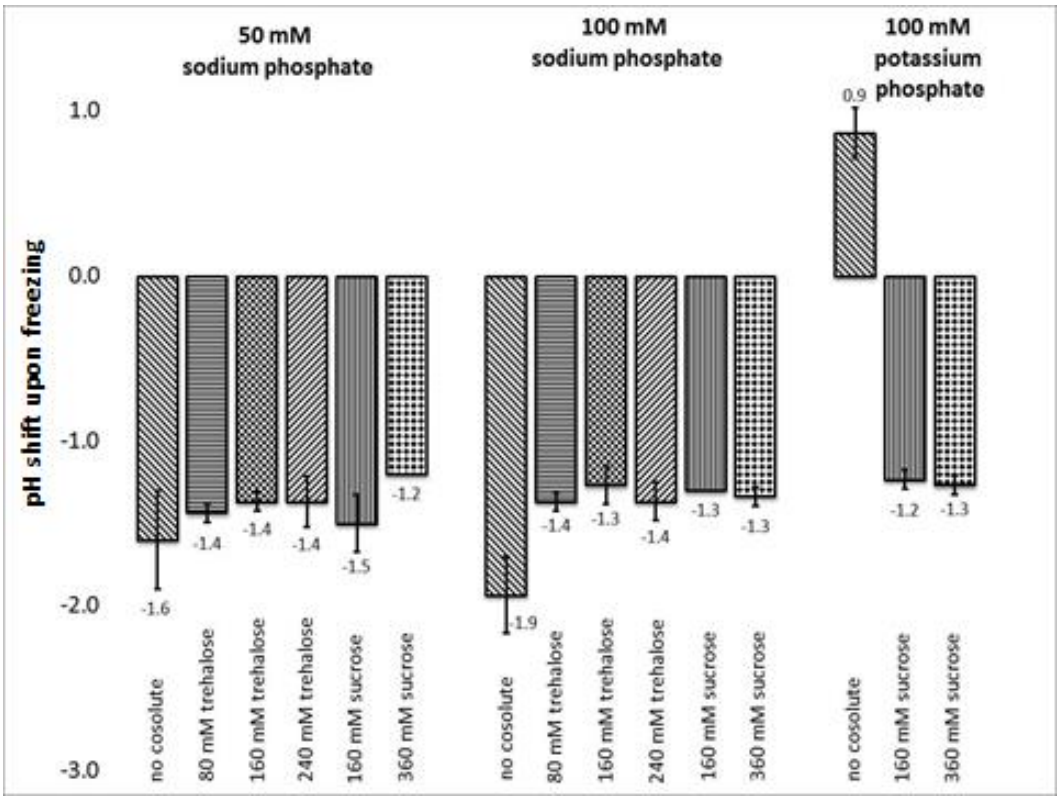

Figure 2.3 pH shifts of frozen phosphate buffer (sodium or potassium) solutions containing sugar (sucrose or trehalose). Each bar shows the magnitude and direction of pH shift. The solutions were cooled from RT to -25 °C at 0.5 °C/min, held for 4 hours and the pH was measured (error bars show standard deviations; n=3).

Since the pH shift is consistently pronounced (> 1 pH unit), the effects of temperature on water ionization, pK_a and activity coefficients of the various species are unlikely to be responsible. In light of the strong propensity of the disodium phosphate to crystallize, it is very unlikely that it will phase separate in the amorphous state. Moreover, we were unable to observe an additional glass transition event attributable to disodium hydrogen phosphate glass. We hypothesize that *the pH changes observed in the absence of buffer*

salt crystallization is brought about by the selective complexation of the dibasic sodium phosphate with sugar (both trehalose and sucrose) in the freeze-concentrate.

2.3.3 Thermal characterization of frozen buffer solutions

The thermal behavior of frozen sucrose solutions has been extensively reviewed in the literature (80). Freeze-concentrated trehalose is characterized by two glass transition temperatures. The reported values of T_g' (the higher temperature transition) ranged from 295.2 – 233.0 K with the experimentally determined trehalose concentration in the maximally freeze-concentrated system (C_g') ranging from 72.0 to 83.3% w/w (74). T_g" values for trehalose have been reported in the range of 228 – 201 K (81, 82). We have determined the T_g' and T_g" of our system (1.1 M trehalose) to be 243.0 and 235.5 K respectively. The respective compositions of the freeze-concentrate (C_g' and C_g") were determined using the Gordon-Taylor equation (Equation 2.2) to be 84.1% and 82.5% w/w trehalose.

$$T'_g = \frac{w_1 T_{g_1} + k w_2 T_{g_2}}{w_1 + k w_2} \qquad \textit{Equation (2.2)}$$

where k = 7.3 (83), T_{g1} (trehalose) = 386.9 K (83), T_{g2} (water) = 138 K (83), T_g' (water-trehalose) = 243 K and T_g" (water-trehalose) = 235.5 K. The trehalose to water ratio for C_g' and C_g" are respectively, 5.3 and 4.7. Thus the "water-rich" phase has ~13% more water than the maximally freeze-concentrated "sugar-rich" phase.

We were next interested in determining the effect of buffer concentration on the glass transition temperatures of freeze-concentrated sugar. Sucrose and trehalose solutions (1.1

M) were buffered to the second pK_a of phosphoric acid (pH=7.2; 25 °C) with buffer concentrations ranging from 0 to 500 mM. The high concentrations were chosen since DSC lacks the sensitivity to discern the glass transitions when the solute concentrations are low. With increasing buffer concentration, in both trehalose and sucrose solutions, T_g' and T_g" decreased linearly though the effect was more pronounced in the latter (Figure 2.4).

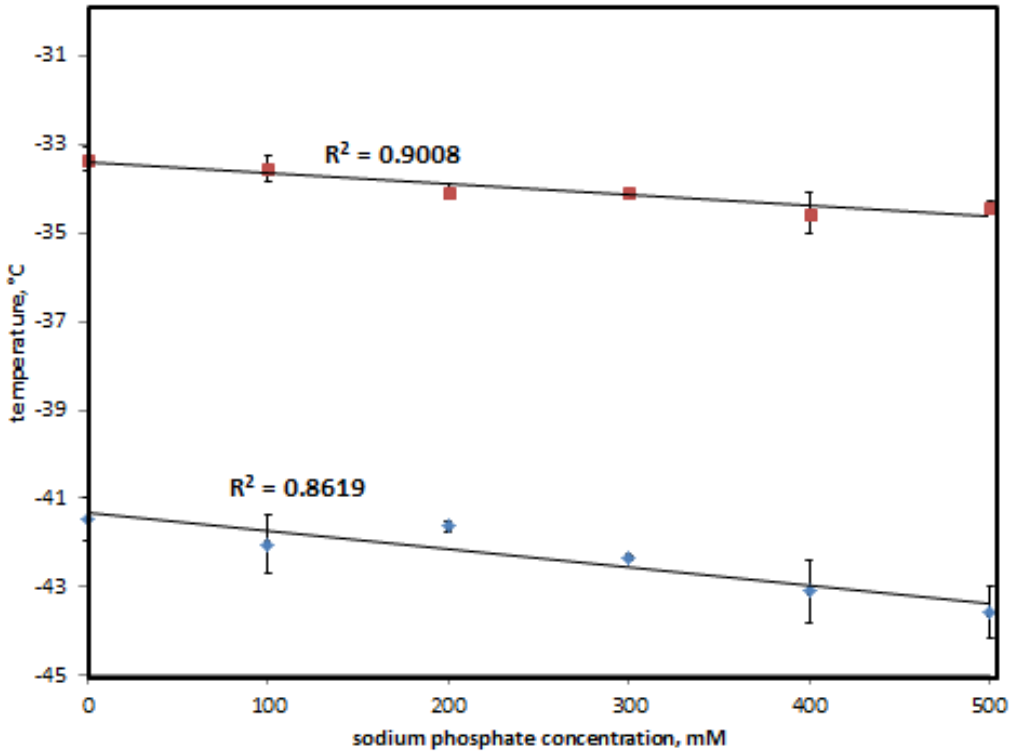

2.4-A: Sucrose

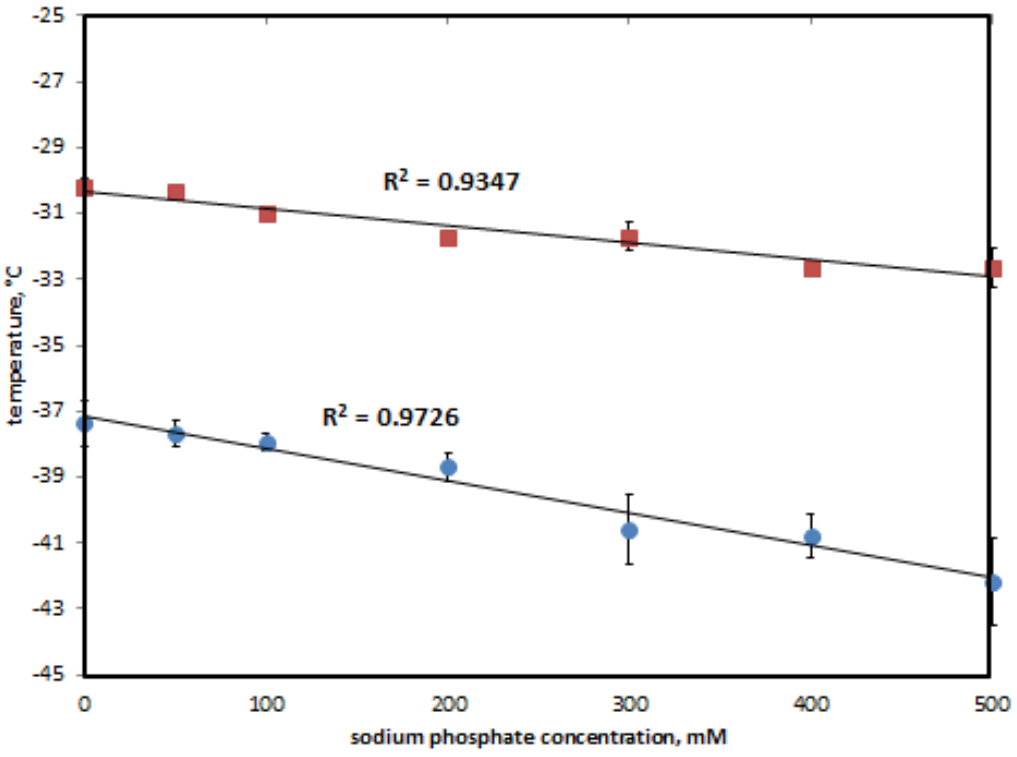

2.4-B: trehalose

Figure 2.4 Plot of the T_g' (the higher temperature transition) and T_g" (the lower temperature transition) of sucrose (A) and trehalose (B) as a function of sodium phosphate concentration.

The glass transition temperatures of the sodium phosphate buffer components are expected to be high (>> RT). A simple empirical rule for strong glasses: $T_m/T_g \leq 1.5$ holds true for inorganic as well as polymeric systems (84). Since the melting temperature of NaH_2PO_4 and Na_2HPO_4 are 463 K and 523 K respectively, the buffer salts are expected to have T_g values substantially higher than ambient temperature. According to the Gordon-Taylor equation (Equation 2.2), the addition of buffer components to the freeze-concentrate will *increase* the T_g' values of both sucrose and trehalose freeze-concentrates. On the other hand, NMR spectroscopy has shown that the decrease

in T_g' upon addition of an electrolyte (sodium chloride or sodium phosphate) is a result of an increase in the unfrozen water content (85). We believe that the same phenomenon is responsible for the observed increase in the glass transition temperatures as a function of buffer concentration. Interestingly, this effect appears to be more pronounced (particularly in trehalose) in the water-rich region (T_g").

So far the starting concentrations of the monobasic and dibasic species were identical (pH = pK_a). As a result, we were unable to discern the effect exerted by the individual buffer components. Therefore, in addition to the intermediate pH values, we now evaluate the effects of the buffer component individually by observing the solution properties at the limits of the buffered pH range. In doing so, the influence of the monosodium phosphate buffer component will be evident at low pH values, while that of disodium phosphate buffer will be apparent at high pH values. Therefore, trehalose solutions (1.1 M) were buffered with sodium phosphate to pH values ranging from 5.7 to 8.7 while the total buffer concentration was maintained at 5 mM. A similar set of solutions were prepared and analyzed with a fixed sodium phosphate concentration of 500 mM.

At low buffer concentration (5 mM), the T_g' and T_g" values were unaffected by solution pH. Therefore the $[HPO_4^{2-}]/[H_2PO_4^-]$ ratio had minimal influence on the glass transition temperature values (Figure 2.5). At low buffer concentrations, the compositions of the water-rich and sugar-rich regions were unaffected by the initial pH.

When the buffer concentration was increased (500 mM), the glass transition temperatures were affected by the initial pH. At high pH values (predominantly disodium phosphate), the glass transition temperatures were unaffected by the presence of buffer. Interestingly, at low pH, an increase in the monosodium phosphate concentration caused a pronounced decrease in both T_g' and T_g". Based on the observed glass transition temperature values at intermediate pH values, it is evident that the concentration of NaH_2PO_4 influences the transition temperatures, in a gradual manner (Figure 2.5). Even at this high buffer concentration (500 mM), there was no evidence of buffer salt crystallization based on DSC (eutectic melting) and FTIR (data not shown).

The progressive decrease in the T_g' and T_g" as the pH is lowered suggests that the NaH_2PO_4 has a greater propensity to interact with water than does Na_2HPO_4. As a result, the freeze-concentrate is more "plasticized" at low pH values (predominantly monosodium phosphate).

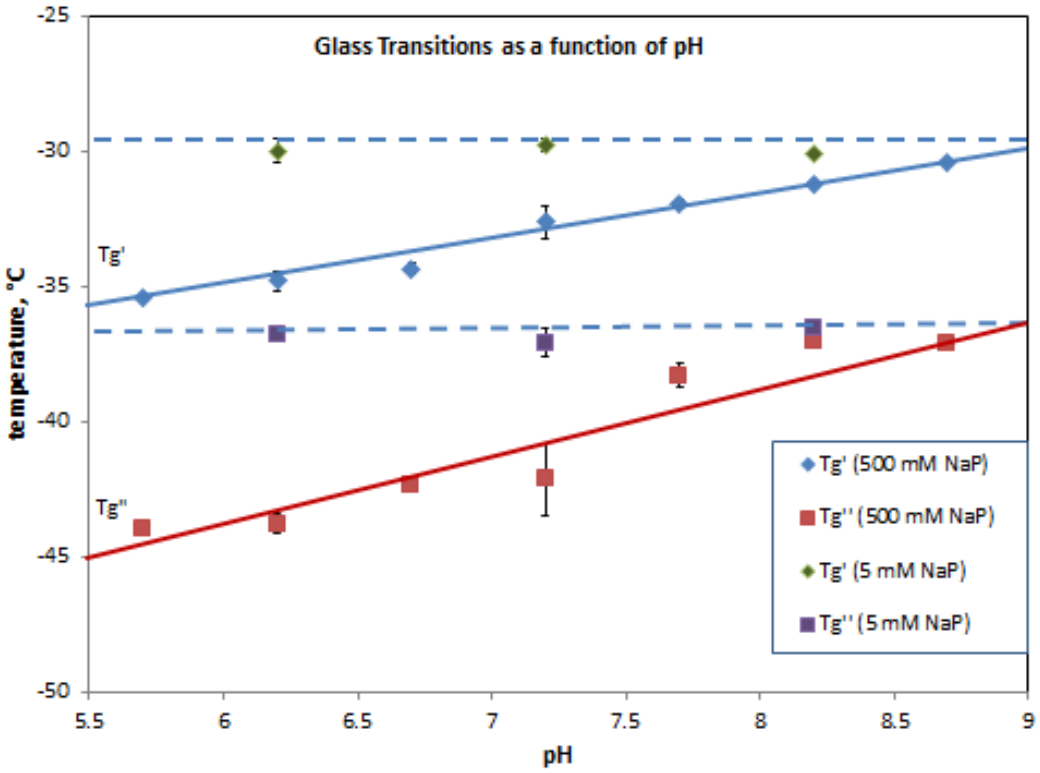

Figure 2.5 T_g' and T_g" are plotted as a function of pH. The blue diamonds (T_g') and red boxes (T_g") represent the transition temperatures of a 1.1 M trehalose, 500 mM sodium phosphate solution. The green diamond (T_g') and purple squares (T_g") represent the transition temperatures of a 1.1 M trehalose, 5 mM sodium phosphate solution. Each sample was tested in triplicate (error bars represent the standard deviations) The samples were cooled in the DSC from 25 °C to -75 °C at 0.1 °C/min. The glass transition temperatures are measured upon warming the frozen systems to 25 °C at 2 °C/min. Dotted lines indicate T_g' and T_g" values of a 1.1 M trehalose (alone) solution. Bold blue and red lines are drawn to assist in visualizing the trends.

2.3.4 Complex Formation

Ohtake et al. documented a 1:1 complex between phosphate and trehalose in freeze-dried systems (79). We now explore the ability of phosphate buffers to form this complex with trehalose in the freeze-concentrate. Using FTIR, we tracked the 1150 cm^{-1}

vibrational peak (sensitive to trehalose conformation) arising from the glycosidic linkage of trehalose. The 1150 cm^{-1} band in the room temperature IR spectrum of a trehalose solution (1 M) was indistinguishable from that of a solution containing trehalose (1M) and sodium phosphate (500 mM) (Figure 2.6). The results show that at room temperature, the phosphate buffer does not influence the frequency of vibration of the glycosidic bond.

When dibasic phosphate is present in the freeze-concentrate, the peaks shift to higher wavelengths indicating an interaction between phosphate and trehalose at subambient temperatures (1 M trehalose, 0.5 M sodium phosphate, pH = 7.2 and 8.2; Figure 2.6). However, when the dibasic phosphate is not present or its concentration is very low, this interaction is not evident [(*i*) 1 M trehalose (alone) and (*ii*) 1 M trehalose, 0.5 M sodium phosphate, pH = 6.2; Figure 2.6]. The interaction is only apparent when the dibasic phosphate form is in abundance (pH $\geq$ pKa) suggesting a highly specific interaction between the dibasic phosphate (HPO_4^{2-}) and trehalose in the freeze-concentrate.

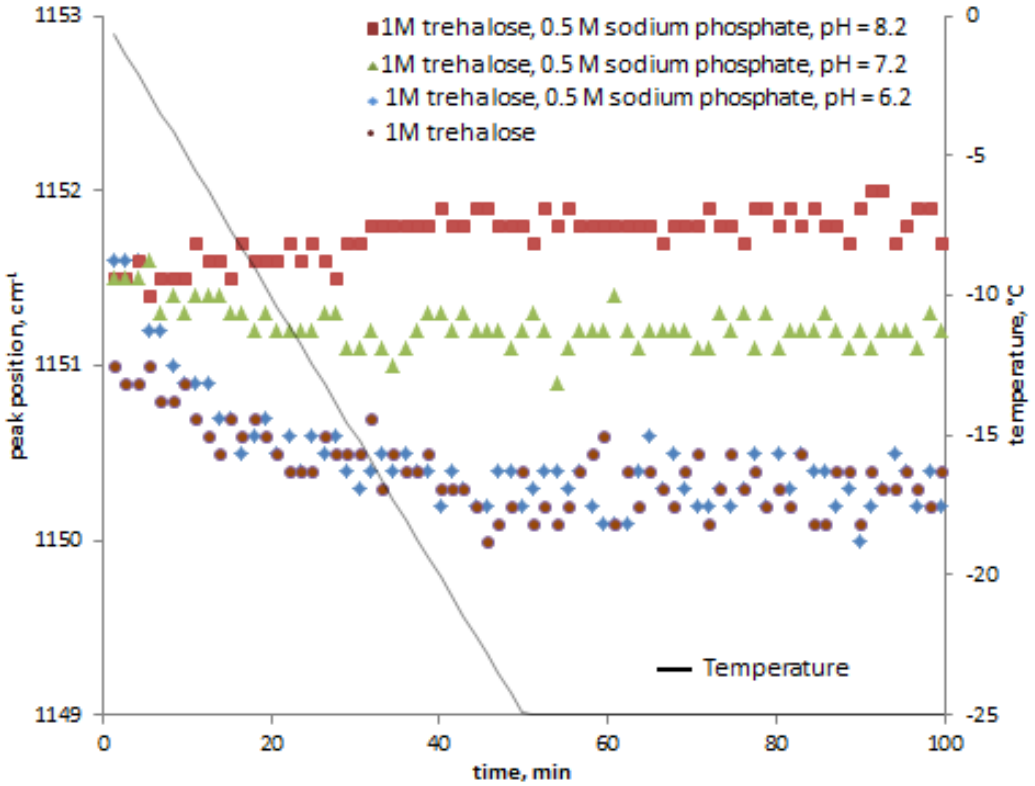

Figure 2.6 Temperature dependence of the trehalose glycosidic vibrational band (1150 cm^{-1}) placement. Shift to lower numbers suggest no complex, while shifts to higher numbers suggest the presence of a phosphate-trehalose complex. Note that there is no difference between a trehalose-only sample (purple) and a trehalose-sodium phosphate, pH = 6.2 solution (blue)

2.4 Discussion

In summary, both the buffer components (monosodium and disodium phosphate) exert a substantial effect on the freeze-concentrate properties. The monosodium phosphate has a greater propensity to interact with water than does Na_2HPO_4. Additionally, the interaction between Na_2HPO_4 and trehalose appears to influence the pK_a of the phosphoric acid. *By altering the pK_a of phosphoric acid, these interactions cause a shift in freeze-concentrate pH without buffer salt crystallization.*

Boric acid, an inorganic acid, forms complexes with both sucrose and trehalose in freeze-concentrated systems (78). This complex is expected to affect the pK_a of boric acid (78). Like borate, phosphate forms a complex with sucrose and trehalose in the dried state (79). The effect of the trehalose-phosphate complex on the pK_a of phosphate will contribute to the apparent change in pH of the freeze-concentrate. The popularity of phosphate buffer stems from one of its pK_a values being close to physiologic pH. The system will exhibit high buffer capacity when the pH is close to the pK_a, i.e. the highest resistance to pH change. The complexation with phosphoric acid, by lowering the pK_a, has the potential to dramatically lower the buffer capacity. Thus the complexation can have two undesirable outcomes: (*i*) alteration in the pH of the freeze-concentrate (and consequent protein destabilization), and (*ii*) decreased ability to resist pH changes.

The existence of "water rich" and "sugar rich" populations in the freeze-concentrate is undesirable since the protein is exposed to two different environments. When the protein

solution is cooled, the cooling rate provides an opportunity to minimize this heterogeneity in the freeze-concentrate. A slower cooling rate is expected to decrease the heterogeneity. This became evident from the pronounced increase in T_g" as the cooling rate was decreased (Figure 2.7). As the system is cooled at a slower rate, there is increased opportunity for the unfrozen water to crystallize and the system is closer to "equilibrium". One can postulate that at an extremely slow (possibly impractical) cooling rate, the T_g" will merge with T_g' yielding a single "population".

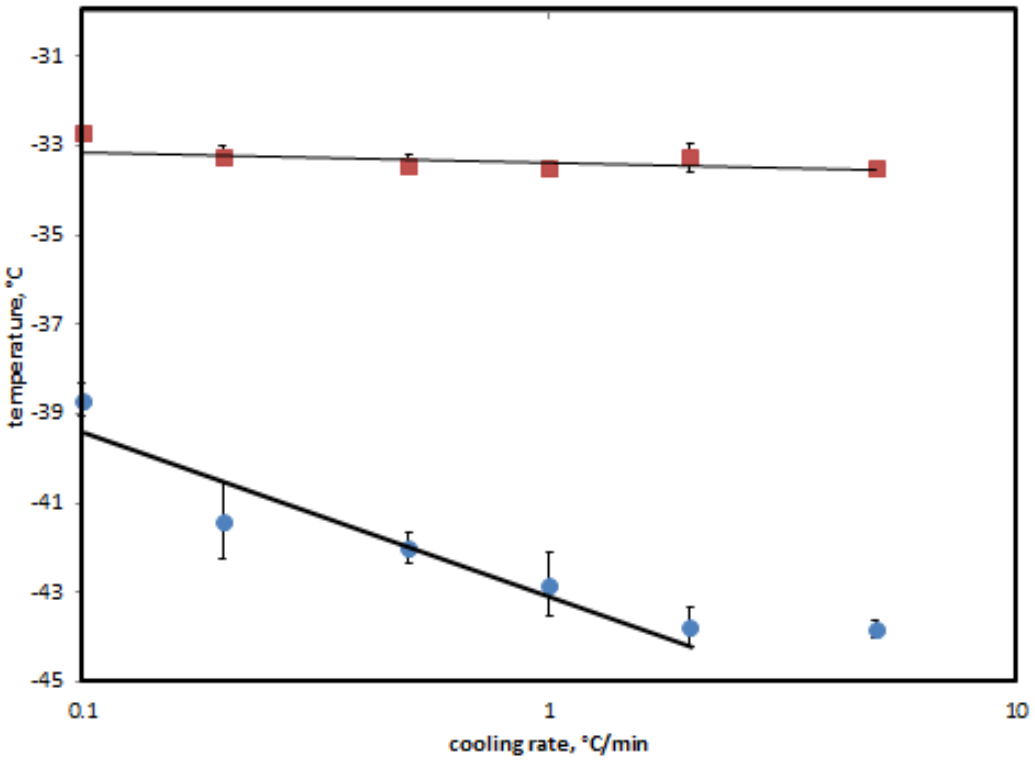

Figure 2.7 Plot of the T_g' (red square) and T_g" (blue circle) of a frozen aqueous solution containing trehalose (1.1 M) and sodium phosphate buffer (500 mM) as a function of cooling rate. The solution pH at RT was 7.2. The solutions were cooled from room temperature to -75 °C at different rates and

then heated to RT at 2 °C/min. The glass transition temperatures were recorded during the heating cycle.

2.5 Significance

To date, in the pharmaceutical community, selective crystallization of a buffer component was believed to be the only mechanism responsible for pH shifts in frozen solutions. Therefore, the buffer selection was based upon (*i*) its ability to remain amorphous (i.e. not crystallize), (*ii*) biocompatibility and (*iii*) providing adequate buffering capability. For the first time, we have documented pronounced pH shifts in freeze-concentrate without any evidence of buffer salt crystallization. This shift was brought about by the interaction between two common excipients (the lyoprotectant and buffer). Pharmaceutical formulators need to consider this potential interaction during the selection of formulation components.

2.6 Acknowledgements

Use of the Advanced Photon Source was supported by the U. S. Department of Energy, Office of Science, Office of Basic Energy Sciences, under Contract No. DE-AC02-06CH11357.

3.0 Characterization of xylitol and evaluation of xylitol as a potential lyoprotectant

3.1 Introduction

Non-reducing sugars such as sucrose and trehalose have been shown to be very effective protein stabilizers in frozen and freeze-dried pharmaceutical formulations.(4, 14, 17, 28, 86) The mechanism of stabilization comes about through a vast network of hydrogen bonds between hydroxyl (-OH) groups on the sugars and oxygen, sulfur and nitrogen molecules on the protein surface.(13, 28) When a compound is able to protect a protein both during freezing and drying, it is referred to as a lyoprotectant. Sucrose and trehalose (both disaccharides) are the only two lyoprotectants currently in use by the pharmaceutical community. However there are limitations with both these sugars. Trehalose has been shown to slowly crystallize during annealing, rendering it unable to protect the active protein,(87) while sucrose will degrade under acidic conditions.(88) The complications from the physical and chemical instabilities of the two available lyoprotectants warrant investigation into novel chemicals with lyoprotective capabilities.

Sugar alcohols are a class of chemicals that are similar to non-reducing sugars. Both sugar alcohols and non-reducing sugars are carbon chains with one hydroxyl group per carbon atom, and thus can also form a large variety of hydrogen bonds. Unlike non-reducing sugars though, sugar alcohols do not form cyclic structures and therefore have greater molecular mobility. Mannitol, a 6-carbon sugar alcohol has been shown to be an excellent lyoprotectant if it is retained amorphous.(89) However, mannitol has a strong tendency to crystallize in frozen systems, limiting its use as a lyoprotectant.(90) Xylitol is a widely available 5-carbon sugar alcohol and unlike mannitol is not expected to

crystallize from a frozen matrix (Figure 3.1).(91, 92) Furthermore, xylitol has been shown to be an effective cryoprotectant (a stabilizer of proteins in frozen solutions), and it is well tolerated when administered parenterally.(93, 94) The aim of this study is to characterize xylitol and to test our hypothesis *that xylitol is an effective lyoprotectant*.

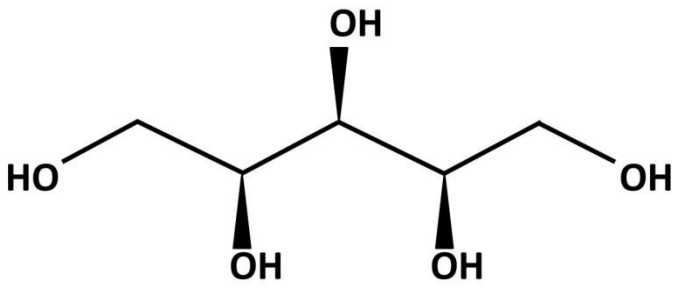

Figure 3.1 Chemical structure of xylitol.

3.2 Methods

3.2.1 Preparation of Buffer Solutions

Buffer solutions were prepared by dissolving the appropriate amount of disodium hydrogen phosphate and other cosolutes, then adjusting the pH to the desired value (± 0.1) with concentrated NaOH (25 °C). The final buffer concentration was 10, 25, 50, 100 or 500 mM. The sugar concentration was fixed at 1 M. All the solutions were membrane filtered (PTFE; 0.45 μm) and used immediately upon preparation.

3.2.2 Differential Scanning Calorimetry

A differential scanning calorimeter (Q2000, TA instruments, New Castle, DE, USA) equipped with a refrigerated cooling accessory was used. The cell constant was

determined using indium and temperature calibration was performed using indium, tin and water as standards. The solutions were transferred by pipette to an aluminum pan and hermetically sealed. The final pan weight was recorded. All the measurements were done under dry nitrogen purge at a heating rate of 2 °C/min.

3.2.3 Synchrotron XRD (Transmission Mode)

The experiments were performed at the synchrotron beam line (6-ID-B, Advanced Photon Source), Argonne National Laboratory (Argonne, IL, USA). The variable temperature stage (High-Tran Cooling System, capable of controlled cooling by using liquid nitrogen) was attached to the Eulerian cradle (Huber 512) using an aluminum plate. An X-ray beam (0.76534 Å; beam size 100 (vertical) × 200 (horizontal) μm) was used, wherein the flux of the incident X-rays (intensity: 1,013 photons/s/mrad^2/mm^2) was attenuated to prevent detector saturation. The monochromator, a triplebounce, channel-cut, [111] faces polished Si single crystal, limited the line broadening to its theoretical low limit, i.e. the Darwin width. An image plate detector (Mar345) with 3,450 × 3,450 pixel resolution in 34.5 mm diameter area, with a readout time of 108 seconds (best resolution mode), was used. The sample to detector distance was set to 500.1 mm. The calibration was performed using a silicon standard (SRM 640b, NIST).

3.2.4 Low Temperature pH Measurements

About 100 ml of solution was placed in a jacketed beaker (250 ml) connected to a water bath with an external controller unit (Neslab RTE 740, Thermo electron, NH). A low

temperature pH electrode (Inlab® cool, Mettler Toledo, Switzerland) was placed in the center of the sample and connected to a pH meter (pH 500 series, Oakton, Singapore) to monitor the electromotive force (EMF), from which the pH of the solution was calculated. Initially, the solutions were allowed to equilibrate at 0 °C, and then cooled to −25 °C at 0.5 °C/min and held at -25 °C for at least 3 hours.

3.2.5 Lyophilization Cycle

Prelyo solution composition was: 20 mM sodium phosphate, 300 mM sugar (sucrose, trehalose or xylitol) and 600 mM mannitol. The lactate dehydrogenase (from Lactobacillus leichmanii, 126.00 activity units/mg solid; purchased from Sigma) was included in the prelyo solution at a concentration of 0.084 mg/ml. The asparginase concentration (from E-coli, 152.36 activity units/mg solid; also purchased from Sigma) was 8.1 µg/ml. The β-galactosidase (from bovine liver, 0.12 activity units/mg solid) was purchased from Sigma-Aldrich and was included in the prelyo solution at a concentration of 0.31 mg/ml. In all systems, the final pH of the prelyo solution was 7.0.

Lyophilization was carried out in a bench-top (VirTis® AdVantage™, Gardiner, NY) freeze-dryer. The prelyo solutions (3 ml) were filled in USP Type I borosilicate glass vials (Wheaton®), with 20 mm neck size and 10 ml fill volume. The freeze-dryer was programmed as follows:

1. Vials were cooled from 25 to -50 °C at 0.25 °C/min.
2. They were annealed at -50 °C for 7 hours.
3. Primary drying was carried out at -50 °C and 70 mTorr for 2 days.

4. Secondary drying was conducted at -10 °C and 70 mTorr for 1 day, then 0 °C and 70 mTorr for 1 day, and finally, 25 °C and 70 mTorr for 1 day.

At the end of the cycle, the vials were capped with rubber stoppers (two-leg gray butyl, Fisher Scientific) under nitrogen gas and then stored in a refrigerator protected from light. The final lyophiles were characterized for elegance and protein activity.

3.2.6 LDH Activity Assay

Lyophilized powders were reconstituted in DI water and stirred with a vortex mixer for 30 seconds to ensure complete dissolution of the solid. Fifty µL of the reconstituted solution was added (in duplicate) to a 96-well plate. Lactate dehydrogenase activity assay kit was purchased from Sigma-Aldrich. Absorption was measured with a UV plate reader (BioTek ELx800) at 405 nm.

3.2.7 β-galactosidase Activity Assay

The assay procedure was substantially similar to that of the LDH assay. Mammalian β-galactosidase Activity Assay kit was purchased from Sigma-Aldrich. Absorption was measured with a UV plate reader (BioTek ELx800) at 405 nm.

3.2.8 L-asparginase Activity Assay

The assay procedure was substantially similar to that of the LDH assay. L-asparginase Activity Assay kit was purchased from BioVision. Absorption was measured with a UV plate reader (BioTek ELx800) at 570 nm.

3.3 Results

In order to promote solution stability, protein formulations often include both amorphous sugars as well as inorganic buffers.(10, 11, 66) Phosphate buffer (sodium salt) is popular for several reasons - its documented use in parenteral formulations, its ability to buffer in the physiological range, its low cost and availability. However, when sodium phosphate-buffered solutions are frozen, a pH shift occurs which has been attributed to the selective crystallization of $Na_2HPO_4 \cdot 12H_2O$.(31, 32, 36) Interestingly, the presence of amorphous sugar can prevent the crystallization of a buffer salt minimizing the detrimental shift in pH.(95) In this paper, xylitol, a 5-carbon sugar alcohol, will be characterized by several analytical techniques (synchrotron XRD, low-temperature pH measurements and DSC) and evaluated for its ability to protect three model proteins (lactate dehydrogenase, β-galactosidase and L-asparginase) in lyophilized formulations.

3.3.1 Synchrotron X-Ray Diffractometry (SXRD)

In order to exert its influence in the formulation, the sugar must interact directly with other molecules in the freeze-concentrate. It must therefore remain dissolved in the freeze-concentrate and not crystallize. In an effort to determine the physical stability of

xylitol under super-cooled conditions, experiments on frozen xylitol solutions were conducted at the Argonne National Laboratory. Figure 3.2 shows a typical result where only ice diffraction rings are observed. The lack of peaks, attributable to xylitol or phosphate buffer, confirms that both components remained amorphous in the freeze-concentrate.

Mannitol, a 6-carbon sugar alcohol has been shown to promote crystallization of solutes from the freeze-concentrate.(96) In an effort to facilitate xylitol crystallization, mannitol was added to a xylitol solution and annealed. Figure 3.3 shows that after 48 hours of annealing at -25 °C, xylitol remained amorphous even as mannitol crystallized. This result clearly demonstrates xylitol's resistance to crystallization as one would expect that crystalline mannitol would, due to its structural similarity to xylitol, help initiate the nucleation of xylitol crystals. By remaining amorphous, xylitol meets the first criterion of lyoprotection.

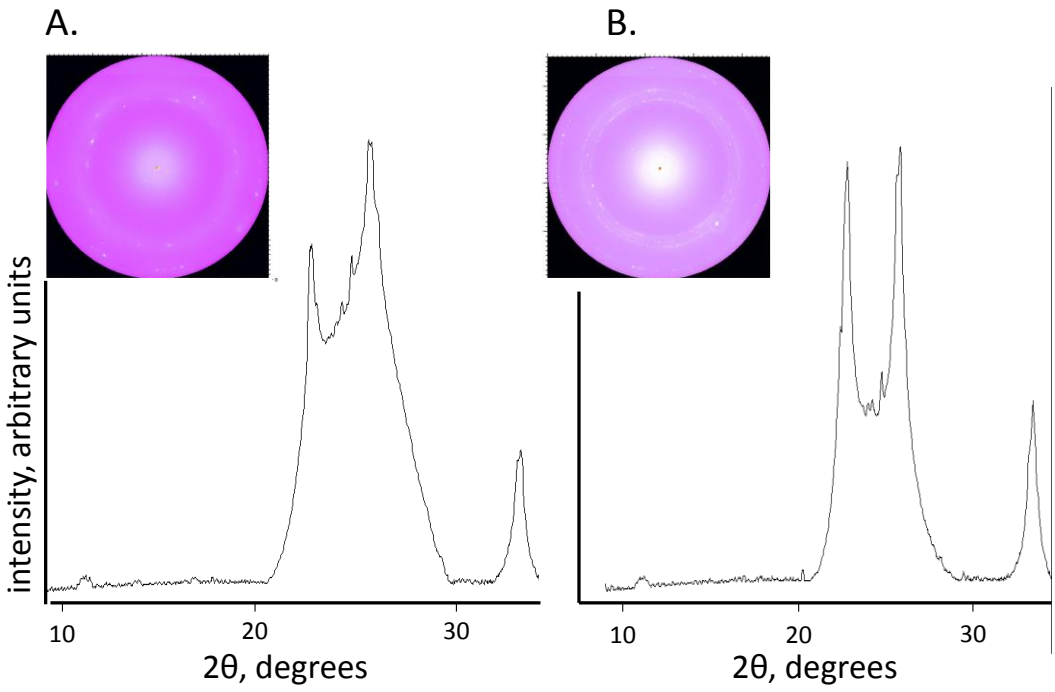

Figure 3.2 Integrated SXRD patterns of frozen and annealed xylitol solutions (inset: raw SXRD images). The solutions were cooled from 0 to -25 °C at 0.5 °C/min and annealed for 48 hours. A. 720 mM xylitol (no buffer); B. 100 mM sodium phosphate, 90 mM xylitol. The peaks observed are all attributable to ice. There was no evidence of xylitol or sodium phosphate crystallization.

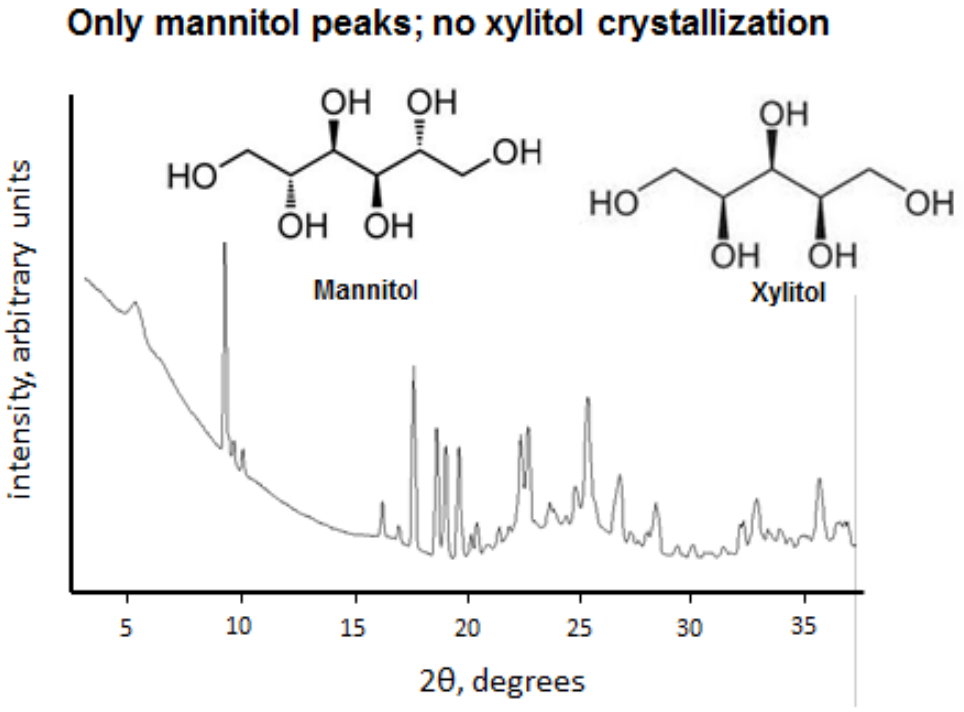

Figure 3.3 SXRD pattern of a frozen and annealed solution containing mannitol (240 mM) and xylitol (360 mM). The solution was cooled from 0 to -25 °C at 0.5 °C/min and annealed for 48 hours. All the peaks are attributable to mannitol hemihydrate.

3.3.2 Low-Temperature pH Measurements

The impact of low (90 mM), medium (180 mM) and high (360 mM) concentrations of xylitol on the pH shift upon freezing of sodium phosphate (10, 25, 50, 100 mM) was investigated. In the absence of xylitol, a sodium phosphate buffered solution (initial pH = 6.2) will shift to lower, acidic pH values by 1.7 – 2.9 pH units (Figure 3.4). The magnitude of pH shift was dependent on initial buffer concentration with the largest pH change observed at the highest initial buffer concentration (100 mM). Even at a low xylitol concentration (90 mM), the pH shift is substantially diminished. At low xylitol

(90 mM) and high buffer concentration (100 mM), the pH shift (decrease) was 1.6 pH units while in the absence of xylitol, the pH change (decrease) of a 100 mM sodium phosphate buffered solution is 2.9 pH units. As the concentration of xylitol increased, the pH shift observed upon freezing was attenuated in a concentration-dependent manner. At high xylitol concentration (360 mM), the pH decrease is ~ 1.0 regardless of the sodium phosphate concentration. When compared to the traditional lyoprotectants, sucrose and trehalose (Figure 3.5), it is evident that xylitol is most effective in attenuating the pH shifts.

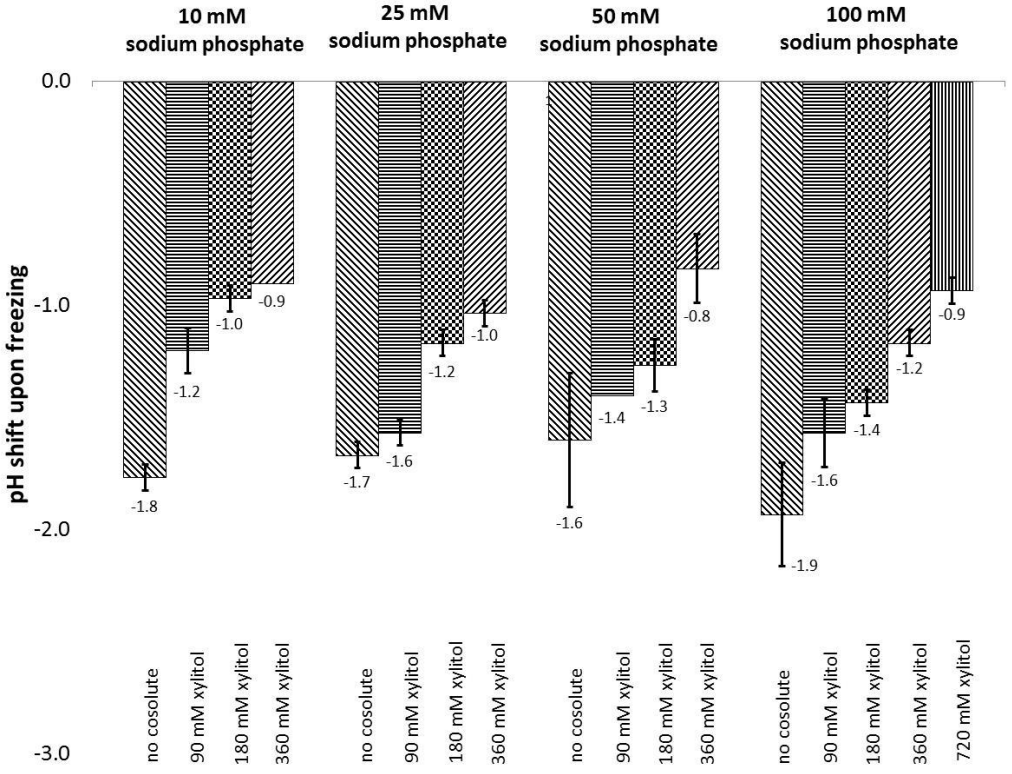

Figure 3.4 The effect of xylitol concentration on the pH shift of frozen sodium phosphate solutions. The buffer solutions were cooled from 0 to -25 °C at 0.5 °C/min and annealed at -25 °C for three

hours. Values represent the largest pH deviation experienced during the cooling and annealing. Error bars represent standard deviations (n=3).

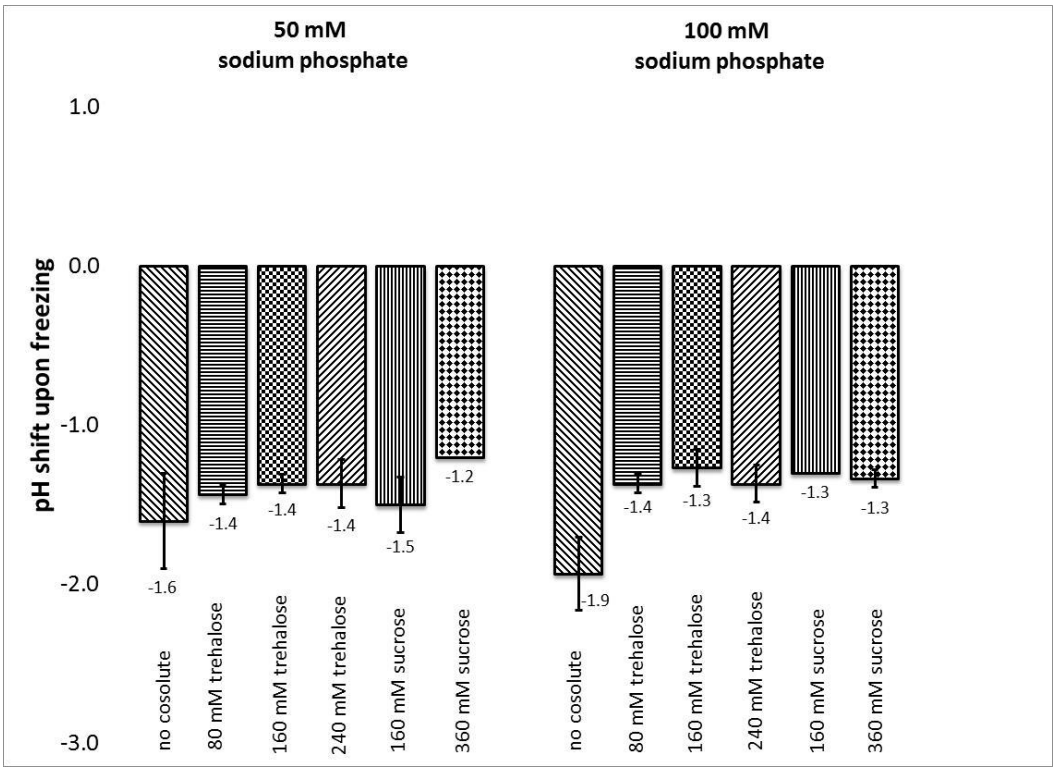

Figure 3.5: The effect of trehalose and sucrose on the pH shift of sodium phosphate buffered solutions.

3.3.3 Differential Scanning Calorimetry

An aqueous solution of xylitol is characterized by two T_g' values. Each of these T_g' values represent a 'separate population' in the freeze-concentrate.(4) The two populations differ in the concentration of xylitol such that the lower value (T_g") represents a more dilute (or water-rich) environment. T_g' was found to be -50.0 ± 1.3 °C while T_g" was -66.6 ± 0.8 °C. Interestingly, upon addition of sodium phosphate (ranging from 100 to 500 mM) to xylitol (concentration fixed at 1.1 M), both the glass transition

values increased with T_g" exhibiting a more pronounced increase than T_g' (Figure 3.6). At the highest buffer concentration (500 mM), the T_g' and T_g" values were respectively -43.3 ± 0.3 °C and -57.2 ± 0.3 °C. The upward trends of both T_g' values are opposite to what was observed with both trehalose and sucrose (data presented in Chapter 2). We had earlier attributed the decrease in T_g' values of trehalose and sucrose with the addition of sodium phosphate to an increase in the amount of unfrozen water in each population. Therefore, the increase in the T_g' values can be explained by a decrease in the unfrozen water content in the freeze-concentrate. We propose that one or both of the sodium phosphate buffer components displace unfrozen water from the freeze-concentrate of a xylitol solution.

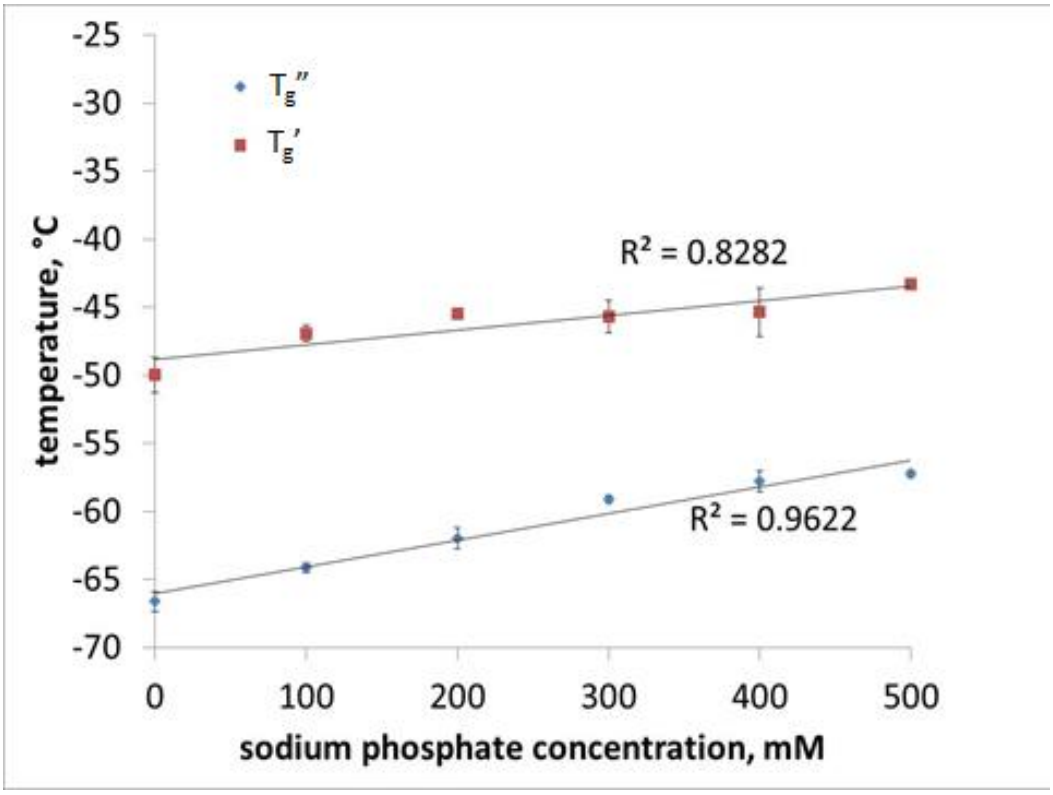

Figure 3.6 The influence of sodium phosphate concentration on glass transition temperature of a freeze-concentrate containing xylitol (fixed at 1.1 M).

Baseline characterization of xylitol has yielded several observations which are highlighted in Figure 3.7. None of these observations preclude xylitol from being a pharmaceutical lyoprotectant (Figure 3.7). Finally, it was necessary to compare the lyoprotection provided by xylitol with that of sucrose and trehalose. Three model proteins, lactate dehydrogenase (LDH), β-galactosidase, and L-asparginase were used for this purpose.

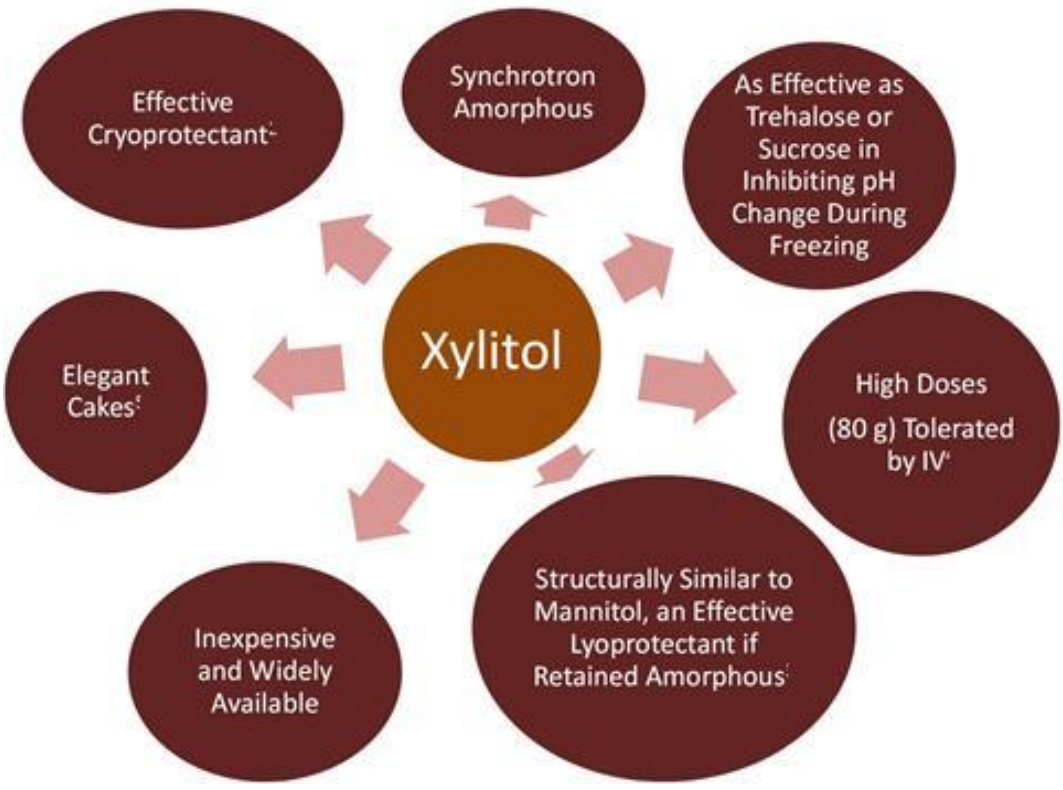

Figure 3.7 Baseline characteristics of xylitol. These properties reveal that xylitol has the potential to be an effective lyoprotectant.

3.3.4 Enzymatic Activity Assays

In an effort to determine the ability of xylitol to perform as a lyoprotectant, three model proteins, lactate dehydrogenase, β-galactosidase, and L-asparginase underwent a complete lyophilization cycle in the presence of a bulking agent (mannitol), a buffer (sodium phosphate, pH = 7.0) and a lyoprotectant (trehalose, sucrose or xylitol). The xylitol containing formulation yielded the most elegant cakes. Unfortunately, as a lyoprotectant, xylitol was not as effective as sucrose or trehalose.

3.3.4.1 Lactate Dehydrogenase

Lactate dehydrogenase served as the first model protein. Upon freeze-drying in the presence of trehalose, 80.7% of the original activity was recovered. Upon freeze-drying in the presence of sucrose, 98.8% of the original activity was recovered. Upon freeze-drying in the presence of xylitol, 79.0% of the original activity was recovered. These results are graphically displayed in Figure 3.8 and show that xylitol is inferior to sucrose and comparable to trehalose in its ability to lyoprotect lactate dehydrogenase.

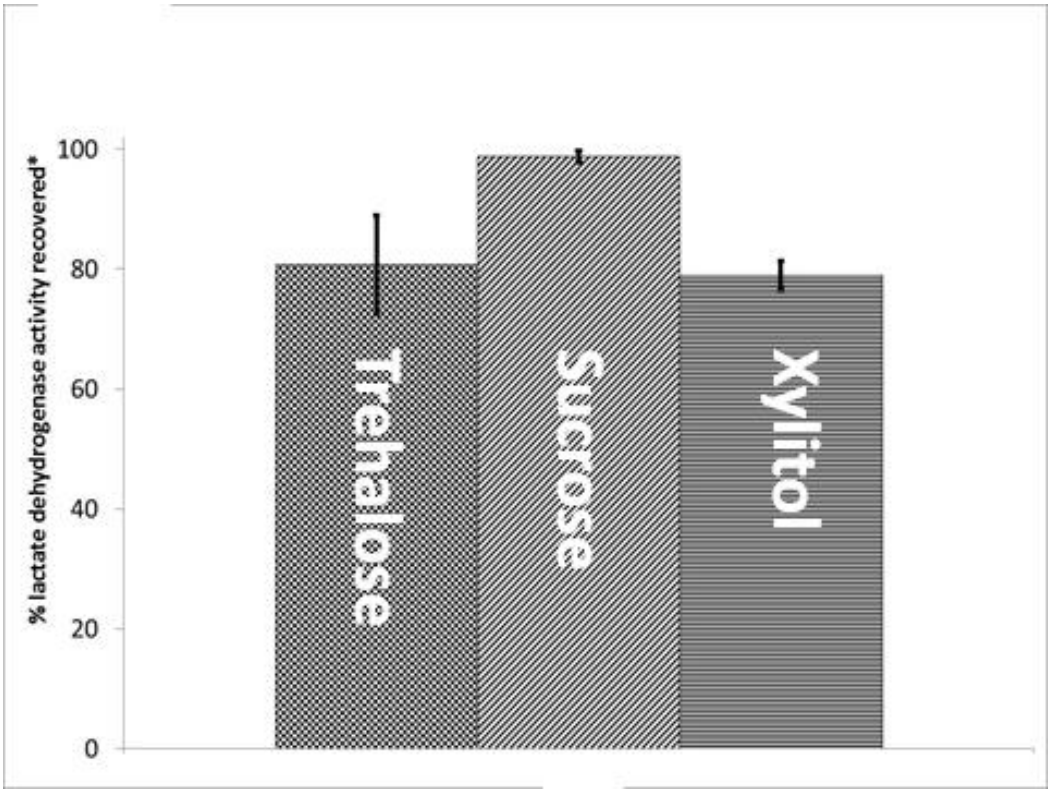

Figure 3.8 Lactate dehydrogenase activity after freeze-drying in the presence of trehalose, sucrose or xylitol. *Activity is compared to the prelyo solution. Error bars represent standard deviations (n = 3).

3.3.4.2 β-galactosidase

β-galactosidase served as the second model protein. Upon freeze-drying in the presence of trehalose, sucrose and xylitol, respectively, 79.3, 89.6 and 43.6% of the original activity was recovered (Figure 3.9). Thus xylitol is inferior to both sucrose and trehalose in its ability to lyoprotect β-galactosidase.

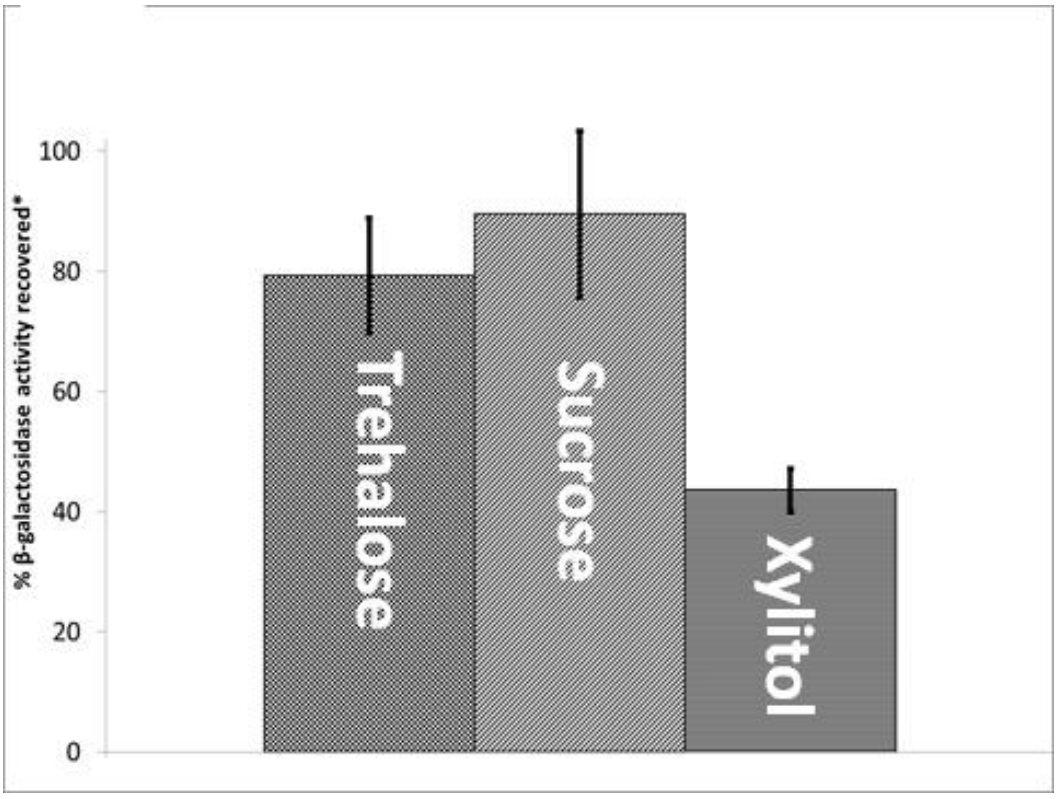

Figure 3.9 β-galactosidase activity after freeze-drying in the presence of trehalose, sucrose or xylitol. *Activity is compared to the prelyo solution. Error bars represent standard deviations (n = 3).

3.3.4.3 L-Asparginase

L-asparginase served as the third and final model protein. Upon freeze-drying in the presence of trehalose, sucrose and xylitol, respectively, 94.5, 93.7 and 84.4% of the

original activity was recovered (Figure 3.10). Thus xylitol is inferior to both sucrose and trehalose in its ability to lyoprotect L-asparginase.

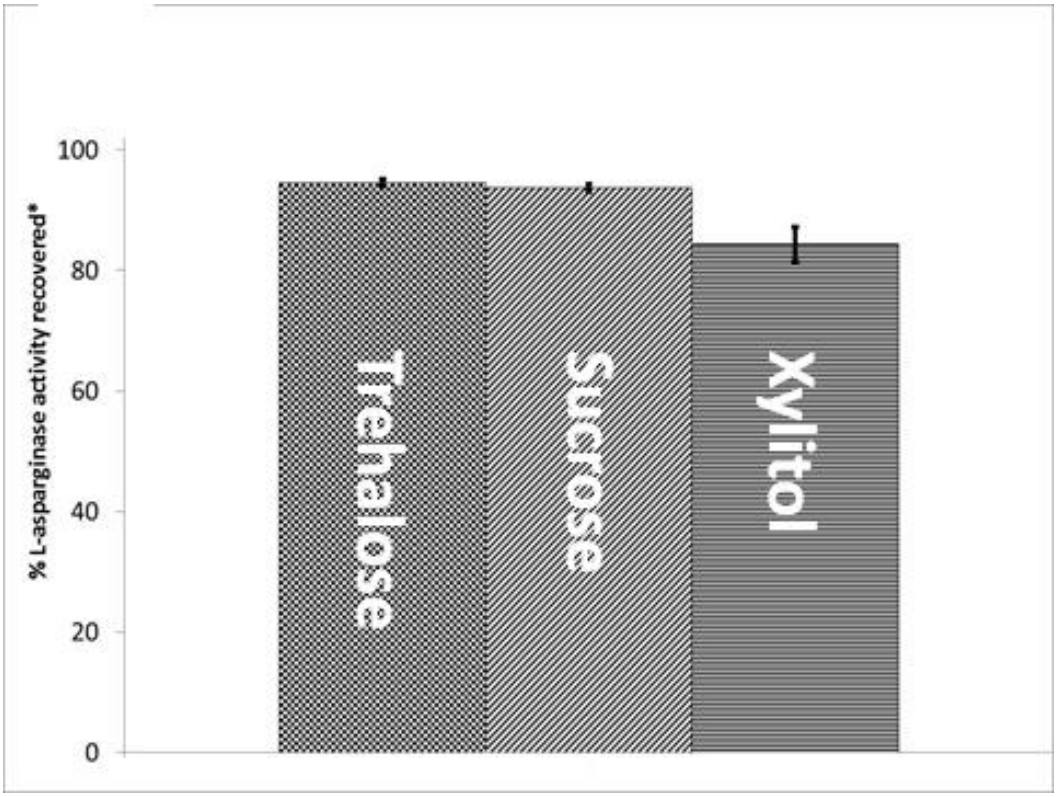

Figure 3.10 L-asparginase activity after freeze-drying in the presence of trehalose, sucrose or xylitol. *Activity is compared to the prelyo solution. Error bars represent standard deviations (n = 3).

3.4 Discussion

Baseline characterization of xylitol revealed its potential to serve as an effective lyoprotectant. Xylitol's effectiveness as a cryoprotectant has been documented.(93) Its effectiveness was compared to that of trehalose and sucrose. Very importantly, xylitol was more effective than either trehalose or sucrose in preventing pH shifts in frozen

solutions. Such shifts have the potential to destabilize proteins and thus this result was especially promising.

Interestingly, the thermal behavior of frozen xylitol solutions was different from that of sucrose or trehalose. While with both sucrose and trehalose, the T_g' and T_g" values decrease with the addition of sodium phosphate buffer, they increase in the case of xylitol (Figure 3.6). The decrease in T_g' values found in trehalose and sucrose have been attributed to an increase in the unfrozen water content in the freeze-concentrate. We therefore attribute the increase in T_g' values of xylitol to be through a mechanism where the addition of sodium phosphate to the freeze-concentrate actually displaces unfrozen water.

Xylitol is a much smaller and more flexible molecule than either trehalose or sucrose (both disaccharides). The smaller size is likely the cause of the low T_g' values found in a super-cooled xylitol solutions, as a small flexible molecule will have greater mobility (all else being equal) than a larger, more rigid non-reducing sugars. It has been well documented that xylitol is an effective cryoprotectant.(93) Thus, based on the theory of preferential exclusion, xylitol is effectively "excluded" from the protein surface in frozen solutions. Since xylitol is not an effective lyoprotectant, we believe that when the frozen solutions are dried, xylitol is not effectively hydrogen bonding and is therefore unable to 'protect' the protein. There is one other possible explanation for xylitol's inability to serve as a lyoprotectant. It may be effectively hydrogen bonding with the protein, but in

light of its small size, the protein surface may be exposed to other formulation components. Thus the denaturation is not brought about because of xylitol's ineffectiveness to hydrogen bond with the protein, but by the other components coming in contact with the protein surface. These issues warrant further investigation and were not the subject of this thesis.

3.5 Significance and practical implications

Currently the pharmaceutical community has only two lyoprotectants at its disposal. Both of these sugars have documented deficiencies highlighting the need for additional lyoprotectants. Initially, xylitol showed great promise in filling this role. Unfortunately, upon actual stability testing with three model proteins, xylitol was the least effective lyoprotectant. Although the freeze-drying community is in need of additional lyoprotectants, xylitol is not a viable candidate.

3.6 Acknowledgements

Use of the Advanced Photon Source was supported by the U. S. Department of Energy, Office of Science, Office of Basic Energy Sciences, under Contract No. DE-AC02-06CH11357.

References:

1. M. Pikal. Freeze-drying of Proteins, Part I: Process design. Biopharm. 3:18-27 (1990).
2. J.L. Cleland, M.F. Powell, and S.J. Shire. The Development of Stable Protein Formulations- A Close Look at Protein Aggregation, Deamidation and Oxidation. Crit Rev Ther Drug. 10:307-377 (1993).
3. J.M. Reichert, C.J. Rosensweig, L.B. Faden, and M.C. Dewitz. Monoclonal antibody successes in the clinic. Nature biotechnology. 23:1073-1078 (2005).
4. B. Bhatnagar, R. Bogner, and M. Pikal. Protein Stability During Freezing: Separation of Stresses and Mechanisms of Protein Stabilization. Pharmaceutical Development and Technology. 12:505-523 (2007).
5. H.R. Constantino. Excipients of Use in Lyophilized Pharmaceutical Peptide, Protein and Other Bioproducts. In H.R. Constantino (ed.), Lyophilization of Biopharmaceuticals, AAPS Press, Arlington, VA, 2004.
6. R.H. Garrett and C.M. Grisham. Principles of Biochemistry With a Human Focus, Thomas Learning Inc., 2002.
7. H.-C. Mahler, W. Friess, U. Grauschopf, and S. Kiese. Protein Aggregation: Pathways, Induction Factors and Analysis. Journal of Pharmaceutical Sciences. 98:2909-2934 (2009).
8. T. Ahern and M.C. Manning (eds.). Stability of Protein Pharmaceuticals: Part B: *In Vivo* Pathways of Degradation and Strategies for Protein Stabilization, Plenum Press, New York, NY, 1992.
9. R. Jaenicke, U. Heber, F. Franks, D. Chapman, M. Griffin, A. Hvidt, and D.A. Cowan. Protein Structure and Function at Low Temperatures [and Discussion]. Philosophical Transactions of the Royal Society of London B, Biological Sciences. 326:535-553 (1990).
10. K.A. Dill. Dominant Forces in Protein Folding. Biochemistry. 29:7133-7155 (1990).
11. A.L. Fink, L.J. Calciano, Y. Goto, T. Kurotsu, and D.R. Palleros. Classification of Acid Denaturation of Proteins: Intermediates and Unfolded States. Biochemistry. 33:12504-12511 (1994).
12. P. Arosio, G. Barolo, T. Müller-Späth, H. Wu, and M. Morbidelli. Aggregation Stability of a Monoclonal Antibody During Downstream Processing. Pharmaceutical Research. 28:1884-1894 (2011).
13. E.Y. Chi, S. Krishnan, T.W. Randolph, and J.F. Carpenter. Physical Stability of Proteins in Aqueous Solution: Mechanism and Driving Forces in Nonnative Protein Aggregation. Pharmaceutical Research. 20:1325-1336 (2003).
14. L. Chang and M.J. Pikal. Mechanisms of Protein Stabilization in the Solid State. Journal of Pharmaceutical Sciences. 98:2886-2908 (2009).

15. J.C. Kasper and W. Friess. The Freezing Step in Lyophilization: Physico-Chemical Fundamentals, Freezing Methods and Consequences on Process Performance and Quality Attributes of Biopharmaceuticals. European Journal of Pharmaceutics and Biopharmaceutics. 78:248-263 (2011).
16. K. Shikama and T. Yamazaki. Denaturation of Catalase by Freezing and Thawing. Nature. 190:83-84 (1961).
17. J.F. Carpenter and J.H. Crowe. The Mechanism of Cryoprotection of Proteins by Solutes. Cryobiology. 25:244-255 (1988).
18. C.A. Angell. Liquid Fragility and the Glass Transition in Water and Aqueous Solutions. Chemical Reviews-Columbus. 102:2627-2650 (2002).
19. S.J. Shire. Formulation and Manufacturability of Biologics. Current Opinion in Biotechnology. 20:708-714 (2009).
20. A. Kantor, S. Tchessalov, and N. Warne. Quality-by-Design for Freeze-Thaw of Biologics: Concepts and Application to Bottles of Drug Substance. American Pharmaceutical Review. 14:65 (2011).
21. S. Duddu and P. Dal Monte. Effect of Glass Transition Temperature on the Stability of Lyophilized Formulations Containing a Chimeric Therapeutic Monoclonal Antibody. Pharmaceutical Research. 14:591-595 (1997).
22. J.A. Searles, J.F. Carpenter, and T.W. Randolph. Annealing to Optimize the Primary Drying Rate, Reduce Freezing-Induced Drying Rate Heterogeneity, and Determine Tg′ in Pharmaceutical Lyophilization. Journal of Pharmaceutical Sciences. 90:872-887 (2001).
23. X. Tang and M. Pikal. Design of Freeze-Drying Processes for Pharmaceuticals: Practical Advice. Pharmaceutical Research. 21:191-200 (2004).
24. J.H. Crowe, J.F. Carpenter, L.M. Crowe, and T.J. Anchordoguy. Are Freezing and Dehydration Similar Stress Vectors? A Comparison of Modes of Interaction of Stabilizing Solutes with Biomolecules. Cryobiology. 27:219-231 (1990).
25. T. Arakawa, Y. Kita, and J. Carpenter. Protein–Solvent Interactions in Pharmaceutical Formulations. Pharmaceutical Research. 8:285-291 (1991).
26. J.F. Carpenter and J.H. Crowe. Modes of Stabilization of a Protein by Organic Solutes During Desiccation. Cryobiology. 25:459-470 (1988).
27. K.R. Ward, G.D.J. Adams, H.O. Alpar, and W.J. Irwin. Protection of the Enzyme l-asparaginase During Lyophilisation—a Molecular Modelling Approach to Predict Required Level of Lyoprotectant. International Journal of Pharmaceutics. 187:153-162 (1999).
28. T. Arakawa and S.N. Timasheff. Stabilization of Protein Structure by Sugars. Biochemistry. 21:6536-6544 (1982).
29. P. Sundaramurthi, T. Patapoff, and R. Suryanarayanan. Crystallization of Trehalose in the Frozen Solutions and its Phase Behavior During Drying. Pharm Res 27:2374-2383 (2010).
30. D.S. Katayama, J.F. Carpenter, K.P. Menard, M.C. Manning, and T.W. Randolph. Mixing Properties of Lyophilized Protein Systems: A Spectroscopic and Calorimetric Study. Journal of Pharmaceutical Sciences. 98:2954-2969 (2009).

31. P. Kolhe, E. Amend, and S. Singh. Impact of Freezing on pH of Buffered Solutions and Consequences for Monoclonal Antibody Aggregation. Biotechnology Progress. 26:727-733 (2010).
32. L. van den Berg and D. Rose. Effect of Freezing on the pH and Composition of Sodium and Potassium Phosphate Solutions: the Reciprocal System KH_2PO_4---Na_2HPO_4---H_2O. Archives of Biochemistry and Biophysics. 81:319-329 (1959).
33. L. van den Berg. The Effect of Addition of Sodium and Potassium Chloride to the Reciprocal System: KH_2PO_4-Na_2HPO_4-H_2O on pH and Composition During Freezing. Archives of Biochemistry and Biophysics. 84:305-315 (1959).
34. N. Murase and F. Franks. Salt Precipitation During the Freeze-Concentration of Phosphate Buffer Solutions. Biophysical Chemistry. 34:293-300 (1989).
35. B.S. Chang and C.S. Randall. Use of Subambient Thermal Analysis to Optimize Protein Lyophilization. Cryobiology. 29:632-656 (1992).
36. G. Gómez, M.J. Pikal, and N. Rodríguez-Hornedo. Effect of Initial Buffer Composition on pH Changes During Far-From-Equilibrium Freezing of Sodium Phosphate Buffer Solutions. Pharmaceutical Research. 18:90-97 (2001).
37. B.A. Szkudlarek. Selective Crystallization of Phosphate Buffer Components and pH Changes During Freezing: Implications to Protein Stability, *Pharmaceutics,* Vol. Ph. D., University of Michigan, 1997.
38. L.J. Henderson. Concerning the Relationship Between the Strength of Acids and Their Capacity to Preserve Neutrality. American Journal of Physiology -- Legacy Content. 21:465 (1908).
39. K.A. Hasselbalch. Die Berechnung der Wasserstoffzahl des Blutes aus der freien und gebundenen Kohlensäure desselben, und die Sauerstoffbindung des Blutes als Funktion der Wasserstoffzahl. Biochemische Zeitschrift. 78:112-144 (1917).
40. H. Galster. pH Measurement, VCH, New York, NY, 1991.
41. G. Gomez. Crystallization-Related pH Changes During Freezing of Sodium Phosphate Buffered Solutions, *Pharmaceutics*, Vol. Ph. D., University of Michigan, 1995.
42. K. Pikal-Cleland, N. Rodríguez-Hornedo, G.L. Amidon, and J.F. Carpenter. Protein Denaturation During Freezing and Thawing in Phosphate Buffer Systems: Monomeric and Tetrameric [beta]-Galactosidase. Archives of Biochemistry and Biophysics. 384:398-406 (2000).
43. P. Sundaramurthi, E. Shalaev, and R. Suryanarayanan. "pH Swing" in Frozen Solutions—Consequence of Sequential Crystallization of Buffer Components. The Journal of Physical Chemistry Letters. 1:265-268 (2009).
44. M. Burcusa, T. Kamerzell, Y. Gokarn, and R. Suryanarayanan. pH Swing in Frozen Phosphate Buffer Solutions, *AAPS National Conference*, New Orleans, LA, 2010.
45. D. Varshney, S. Kumar, E. Shalaev, S.-W. Kang, L. Gatlin, and R. Suryanarayanan. Solute Crystallization in Frozen Systems–Use of Synchrotron Radiation to Improve Sensitivity. Pharmaceutical Research. 23:2368-2374 (2006).
46. D. Varshney, P. Sundaramurthi, S. Kumar, E. Shalaev, S.-W. Kang, L. Gatlin, and R. Suryanarayanan. Phase Transitions in Frozen Systems and During Freeze–

Drying: Quantification Using Synchrotron X-Ray Diffractometry. Pharmaceutical Research. 26:1596-1606 (2009).
47. D. Varshney, S. Kumar, E. Shalaev, P. Sundaramurthi, S.-W. Kang, L. Gatlin, and R. Suryanarayanan. Glycine Crystallization in Frozen and Freeze-dried Systems: Effect of pH and Buffer Concentration. Pharmaceutical Research. 24:593-604 (2007).
48. J.W. Mullin. Crystallization, Elsevier Science, 2001.
49. W. Kauzmann. The Nature of the Glassy State and the Behavior of Liquids at Low Temperatures. Chemical Reviews. 43:219-256 (1948).
50. L.S. Taylor and S.L. Shamblin. Amorphous Solids. Polymorphism in Pharmaceutical Solids, pp. 587-630.
51. J.H. Gibbsand E.A. DiMarzio. Nature of the Glass Transition and the Glassy State. The Journal of Chemical Physics. 28:373-383 (1958).
52. C. Inoue and T. Suzuki. Enthalpy Relaxation of Freeze Concentrated Sucrose–Water Glass. Cryobiology. 52:83-89 (2006).
53. J. Wu, M. Reading, and Q. Duncan. Application of Calorimetry, Sub-Ambient Atomic Force Microscopy and Dynamic Mechanical Analysis to the Study of Frozen Aqueous Trehalose Solutions. Pharmaceutical Research. 25:1396-1404 (2008).
54. J.M. Gordon, G.B. Rouse, J.H. Gibbs, and J.W.M. Risen. The composition dependence of glass transition properties. The Journal of Chemical Physics. 66:4971-4976 (1977).
55. V. Velikov, S. Borick, and C.A. Angell. The Glass Transition of Water, Based on Hyperquenching Experiments. Science. 294:2335-2338 (2001).
56. B.C. Hancock and G. Zografi. The Relationship Between the Glass Transition Temperature and the Water Content of Amorphous Pharmaceutical Solids. Pharmaceutical Research. 11:471-477 (1994).
57. R.H.M. Hatleyand F. Franks. Applications of DSC in the development of improved freeze-drying processes for labile biologicals. Journal of Thermal Analysis. 37:1905-1914 (1991).
58. W.W. Wendlandt. Thermal analysis, Wiley, 1986.
59. R. Silverstein and F. Webster. Spectrometric Identification of Organic Compounds, John Wiley & Sons, 2006.
60. J. Joseph and E. Jemmis. Red-, Blue-, or No-Shift in Hydrogen Bonds: A Unified Explanation. Journal of the American Chemical Society. 129:4620-4632 (2007).
61. W.F. Wolkers, A.E. Oliver, F. Tablin, and J.H. Crowe. A Fourier-Transform Infrared Spectroscopy Study of Sugar Glasses. Carbohydrate Research. 339:1077-1085 (2004).
62. W.F. Wolkers, H. Oldenhof, M. Alberda, and F.A. Hoekstra. A Fourier Transform Infrared Microspectroscopy Study of Sugar Glasses: Application to Anhydrobiotic Higher Plant Cells. Biochimica et Biophysica Acta (BBA)-General Subjects. 1379:83-96 (1998).
63. B.B. He. Introduction to Two-Dimensional X-Ray Diffraction. Powder Diffraction. 18:71-85 (2003).

64. R. Jenkins and R. Snyder. Introduction to X-Ray Powder Diffractometry, John Wiley & Sons, Inc., New York, NY, 1996.
65. B.B. He. Two-dimensional X-Ray Diffraction, John Wiley & Sons, 2011.
66. F. Jameel and M. Pikal. Design of a Formulation for Freeze Drying. In J.a. Hershenson (ed.), Formulation and Process Development Strategies for Manufacturing Biopharmaceuticals, John Wiley & Sons Inc., 2010.
67. K.A. Pikal-Cleland, N. Rodríguez-Hornedo, G.L. Amidon, and J.F. Carpenter. Protein Denaturation During Freezing and Thawing in Phosphate Buffer Systems: Monomeric and Tetrameric [beta]-Galactosidase. Archives of Biochemistry and Biophysics. 384:398-406 (2000).
68. P. Sundaramurthi and R. Suryanarayanan. Calorimetry and Complementary Techniques to Characterize Frozen and Freeze-Dried Systems. Advanced Drug Delivery Reviews. 64:384-395 (2012).
69. P. Sundaramurthi, E. Shalaev, and R. Suryanarayanan. "pH Swing" in Frozen Solutions-Consequence of Sequential Crystallization of Buffer Components. Journal of Physical Chemistry Letters. 1:265-268 (2010).
70. M. Burcusa, V. Ragoonanan, A. Aksan, and R. Suryanarayanan. Use of Spectroscopic Techniques to Characterize Microheterogeneity in the Freeze-Concentrate of Trehalose-Sodium Phosphate Solutions, *AAPS*, Chicago, IL, 2012.
71. L. Chang, N. Milton, D. Rigsbee, D.S. Mishra, X. Tang, L.C. Thomas, and M.J. Pikal. Using Modulated DSC to Investigate the Origin of Multiple Thermal Transitions in Frozen 10% Sucrose Solutions. Thermochimica Acta. 444:141-147 (2006).
72. H. Levine and L. Slade. Thermomechanical Properties of Small-Carbohydrate–Water Glasses and 'Rubbers'. Kinetically Metastable Systems at Sub-Zero Temperatures. J Chem Soc, Faraday Trans 1. 84:2619-2633 (1988).
73. G. Sacha and S. Nail. Thermal Analysis of Frozen Solutions: Multiple Glass Transitions in Amorphous Systems. Journal of Pharmaceutical Sciences. 98:3397-3405 (2009).
74. T. Chen, A. Fowler, and M. Toner. Literature Review: Supplemented Phase Diagram of the Trehalose–Water Binary Mixture. Cryobiology. 40:277-282 (2000).
75. K. Izutsu, A. Rimando, N. Aoyagi, and S. Kojima. Effect of Sodium Tetraborate (Borax) on the Thermal Properties of Frozen Aqueous Sugar and Polyol Solutions. Chemical and Pharmaceutical Bulletin. 51:663-666 (2003).
76. D.P. Miller, R.E. Anderson, and J.J. de Pablo. Stabilization of Lactate Dehydrogenase Following Freeze-Thawing and Vacuum-Drying in the Presence of Trehalose and Borate. Pharmaceutical Research. 15:1215-1221 (1998).
77. K.A. Connors and J.M. Lipari. Effect of Cycloamyloses on Apparent Dissociation Constants of Carboxylic Acids and Phenols: Equilibrium Analytical Selectivity Induced by Complex Formation. Journal of Pharmaceutical Sciences. 65:379-383 (1976).

78. M. Longinotti and H. Corti. Electrical Conductivity and Complexation of Sodium Borate in Trehalose and Sucrose Aqueous Solutions. Journal of Solution Chemistry. 33:1029-1040 (2004).
79. S. Ohtake, C. Schebor, S.P. Palecek, and J.J. de Pablo. Effect of pH, Counter Ion, and Phosphate Concentration on the Glass Transition Temperature of Freeze-Dried Sugar-Phosphate Mixtures. Pharmaceutical Research. 21:1615-1621 (2004).
80. Y. Roos and M. Karel. Phase Transitions of Amorphous Sucrose and Frozen Sucrose Solutions. Journal of Food Science. 56:266-267 (1991).
81. A. Pyne, R. Surana, and R. Suryanarayanan. Enthalpic Relaxation in Frozen Aqueous Trehalose Solutions. Thermochimica Acta. 405:225-234 (2003).
82. N. Ekdawi-Sever, L.A. Goentoro, and J.J. De Pablo. Effects of Annealing on Freeze-Dried Lactobacillus acidophilus. Journal of Food Science. 68:2504-2511 (2003).
83. L.M. Crowe, D.S. Reid, and J.H. Crowe. Is Trehalose Special for Preserving Dry Biomaterials? Biophysical Journal. 71:2087-2093 (1996).
84. S. Sakka and J.D. Mackenzie. Relation Between Apparent Glass Transition Temperature and Liquids Temperature for Inorganic Glasses. Journal of Non-Crystalline Solids. 6:145-162 (1971).
85. L.-M. Her, M. Deras, and S.L. Nail. Electrolyte-Induced Changes in Glass Transition Temperatures of Freeze-Concentrated Solutes. Pharmaceutical Research. 12:768-772 (1995).
86. T. Arakawa, S.J. Prestrelski, W.C. Kenney, and J.F. Carpenter. Factors Affecting Short-Term and Long-Term Stabilities of Proteins. Advanced Drug Delivery Reviews. 46:307-326 (2001).
87. P. Sundaramurthi and R. Suryanarayanan. Trehalose Crystallization During Freeze-Drying: Implications on Lyoprotection. Journal of Physical Chemistry Letters. 1:510-514 (2010).
88. M. Del Pilar Buera, J. Chirife, and M. Karel. A Study of Acid-Catalyzed Sucrose Hydrolysis in an Amorphous Polymeric Matrix at Reduced Moisture Contents. Food Research International. 28:359-365 (1995).
89. K. Izutsu, S. Yoshioka, and T. Terao. Effect of Mannitol Crystallinity on the Stabilization of Enzymes during Freeze-Drying. Chem Pharm Bull. 42:5-8 (1994).
90. X. Liao, R. Krishnamurthy, and R. Suryanarayanan. Influence of Processing Conditions on the Physical State of Mannitol—Implications in Freeze-Drying. Pharmaceutical Research. 24:370-376 (2007).
91. L. Carpentier, S. Desprez, and M. Descamps. Crystallization and Glass Properties of Pentitols. Journal of Thermal Analysis & Calorimetry. 73:577-586 (2003).
92. K.K. Makinen and E. Soderllng. A Quantitative Study of Mannitol, Sorbitol, Xylitol and Xylose in Wild Beries and Commercial Fruits. Journal of Food Science. 45:367-371 (1980).
93. J.F. Carpenter, J.H. Crowe, and T. Arakawa. Comparison of Solute-Induced Protein Stabilization in Aqueous Solution and in the Frozen and Dried States. Journal of Dairy Science. 73:3627-3636 (1990).

94. A.F. Leutenegger, H. Göschke, K. Stutz, H. Mannhart, D. Werdenberg, G. Wolff, and M. Allgöwer. Comparison Between Glucose and a Combination of Glucose, Fructose, and Xylitol as Carbohydrates for Total Parenteral Nutrition of Surgical Intensive Care Patients. The American Journal of Surgery. 133:199-205 (1977).
95. P. Sundaramurthi and R. Suryanarayanan. The Effect of Crystallizing and Non-crystallizing Cosolutes on Succinate Buffer Crystallization and the Consequent pH Shift in Frozen Solutions. Pharmaceutical Research. 28:374-385 (2011).
96. P. Sundaramurthi and R. Suryanarayanan. Influence of Crystallizing and Non-Crystallizing Cosolutes on Trehalose Crystallization During Freeze-Drying. Pharm Res. 27:2384-2393 (2010).